AOS Thesis

Searching for New Genes That Cause Usher Syndrome

ALA MOSHIRI[#], NIUSHA KASIRI[#], MICHAEL SHEA, LAYLA ALI, BENJAMIN YANG, ANDY SHAO, DAVE CLARY, ANN M. FLENNIKEN, MOHAMMAD ESKANDARIAN, OANA V. AMARIE, LORE BECKER, RICCARDO SANGERMANO, EMILY M. PLACE, KINGA M. BUJAKOWSKA, RACHEL M. HUCKFELDT, ZORANA BERBEROVIC, RAPHAËL BOUR, FABRICE RIET, STEVE D. BROWN, ABIGAIL D'SOUZA, HELMUT FUCHS, VALERIE GAILUS-DURNER, ALAIN GUIMOND, YANN HÉRAULT, MARTIN HRABĚ DE ANGELIS, ALINE LUX, CHRISTOPHE MITTELHAEUSER, LAURYL M.J. NUTTER, MARCELA PALKOVA, JIRI LINDOVSKY, BENOIT PETIT-DEMOULIERE, JAN PROCHAZKA, VIVIAN BRADASCHIA, LOIS KELSEY, COLIN MCKERLIE, MILES JOSEPH RAISHBROOK, RADISLAV SEDLACEK, THE INTERNATIONAL MOUSE PHENOTYPING CONSORTIUM, LOUISE LANOUE, K.C. KENT LLOYD, MICHEL J. ROUX, AND OLIVIA BERMINGHAM-MCDONOGH

• PURPOSE: The purpose of this project was to identify novel Usher syndrome (USH) candidate genes from phenotyping data of 9139 knockout (KO) mouse lines.

• METHODS: We evaluated phenotype data for concurrent retinopathy and hearing abnormalities in single-gene KO mice generated by the International Mouse Phenotyping Consortium (IMPC). A search was performed to determine whether each gene had been previously associated with retinopathy and/or deafness in humans. Bioinformatic tools were used to predict protein interactions, molecular functions, signaling pathways, and the expression of human orthologues of candidate genes in the retina and inner ear.

• RESULTS: We identified 18 single-gene KO lines exhibiting hearing abnormality and retinopathy after ear and eye examinations, respectively, and/or by histopathology. The molecular functions and signaling pathways of the human orthologues of the 18 candidate genes partially overlapped with those of USH genes. Particularly, FER and DYRK1B proteins were predicted to interact with proteins encoded by known ciliopathy genes. *ADIPOR1*, *ATP8B1*, and *MPDZ* were associated with retinal degeneration in humans. *CHSY1* and *IDUA* may be pathogenic causes of hearing impairment in people. Furthermore, *CHSY1*, *CSTB*, and *SPRED1* were located adjacent to unsolved genetic loci related to USH.

• CONCLUSIONS: A screen of 9139 KO mouse lines revealed 18 candidate genes exhibiting both retinal and inner ear abnormalities consistent with the principal clinical features associated with USH. As the observed phenotypes are attributed to gene deletion in mice, these genes warrant further study to determine the causation of retinal degeneration and hearing loss in patients. (Am J Ophthalmol 2026;290: 258–276. © 2026 The Authors. Published by Elsevier Inc. This is an open access article under the CC BY license (http://creativecommons.org/licenses/by/4.0/))

AJO.com Supplemental Material available at AJO.com.

NOTE: Publication of this article is sponsored by the American Ophthalmological Society.

Accepted for publication June 8, 2026.

Department of Ophthalmology and Vision Science (A.M., N.K., M.S., B.Y., A.S.), School of Medicine, University of California-Davis, Davis, California, USA; College of Medicine, California Northstate University (L.A.), California, USA; Mouse Biology Program, University of California—Davis (D.C., L.L., K.C.K.L.), Davis, California, USA; The Centre for Phenogenomics, The Hospital for Sick Children (A.M.F., M.E., Z.B., A.D., L.M.J.N., V.B., L.K.), Toronto, Ontario, Canada; Lunenfeld-Tanenbaum Research Institute, Mount Sinai Hospital (A.M.F., M.E., Z.B., A.D., V.B., L.K.), Toronto, Ontario, Canada; Institute of Experimental Genetics and German Mouse Clinic (O.V.A., L.B., H.F., V.G.-D., M.H.d.A.), Helmholtz Munich, Neuherberg, Germany; Ocular Genomics Institute, Massachusetts Eye and Ear, Department of Ophthalmology, Harvard Medical School (R.S., E.M.P., K.M.B., R.M.H.), Boston, Massachusetts, USA; Université de Strasbourg, CNRS UMR 7104, INSERM U 1258, IGBMC, Institut Clinique de la Souris, PHENOMIN (R.B., F.R., A.G., Y.H., A.L., C.M., B.P.-D.), Illkirch-Graffenstaden, France; Medical Research Council, Harwell Institute (S.D.B.), Harwell, UK; German Center for Diabetes Research (DZD) (M.H.d.A.), Neuherberg, Germany; Chair of Experimental Genetics, TUM School of Life Sciences, Technische Universität München (M.H.d.A.), Freising, Germany; Program in Genetics and Genome Biology (L.M.J.N.), The Hospital for Sick Children, Toronto, ON, M5G 1 X8, Canada; Czech Centre for Phenogenomics, Institute of Molecular Genetics of the Czech Academy of Sciences (M.P., J.L., J.P., M.J.R., R.S.), Vestec, Czech Republic; Translational Medicine, The Hospital for Sick Children (C.M.), Toronto, Ontario, Canada; Department of Laboratory Medicine and Pathobiology, Faculty of Medicine, University of Toronto (C.M.), Toronto, Ontario, Canada; Department of Surgery, School of Medicine, University of California—Davis (K.C.K.L.), Sacramento, California, USA; Institut de Génétique et de Biologie Moléculaire et Cellulaire, Université de Strasbourg (Y.H., M.J.R.), Illkirch, France; Department of Neurobiology and Biophysics, University of Washington School of Medicine (O.B.-M.), Seattle, Washington, USA

Inquiries to Ala Moshiri, Department of Ophthalmology and Vision Science, School of Medicine, UC Davis Eye Center, Ernest E. Tschannen Eye Institute, 4860 Y. Street, Suite 2400, Sacramento, California 95817, USA; e-mail: amoshiri@health.ucdavis.edu

[#] These authors are co-first authors and contributed equally to this work.

© 2026 The Authors. Published by Elsevier Inc.
This is an open access article under the CC BY license
(http://creativecommons.org/licenses/by/4.0/)

0002-9394/$36.00
https://doi.org/10.1016/j.ajo.2026.06.016

INTRODUCTION

The combination of vision and hearing loss, referred to as dual sensory impairment (DSI), can be caused by widely different conditions and affects 11.3% of the United States population aged 80 years and older.[1] Congenital forms of DSI are often heritable single-gene disorders, such as Usher syndrome (USH), Bardet-Biedl syndrome (BBS), Stickler syndrome, Waardenburg syndrome, Alstrom disease, Tietz albinism-deafness syndrome, Norrie disease, Charge syndrome, Alport syndrome, and mitochondrial DNA disorders, such as Kearns-Sayre syndrome and maternally inherited diabetes and deafness.[2] USH has a prevalence of 1 to 4 in 25,000 individuals and is the most common DSI phenotype.[3]

USH is an autosomal recessive (AR) condition affecting the photoreceptors in the retina and the hair cells (HCs) of the cochlea and vestibule in the inner ear, resulting in retinitis pigmentosa (RP), sensorineural hearing loss (SNHL), and variable vestibular dysfunction.[4] Symptoms and signs of USH have different severities and onsets and are categorized into 4 main clinical types (USH1, USH2, USH3, USH4).[2] Pathogenic variants in 10 different genes are associated with USH: *MYO7A*, *USH1C*, *CDH23*, *PCDH15*, and *USH1G* for USH1; *USH2A*, *ADGRV1*, and *WHRN* for USH2; *CLRN1* for USH3; and *ARSG* for USH4.[2] The association of 5 additional genes (*ABHD12*, *CEP250*, *CEP78*, *ESPN*, and *PDZD7*) related to this syndrome remains unclear.[2,5,6] Furthermore, there are likely additional genes at 3 genomic loci mapped to USH1,:10p11.21 to q21.1, 15q22 to q23, and 21q21,[2,6] confirming that unknown USH genes could exist.

Structural USH proteins in the inner ear are organized into major complexes that are essential for the function and stability of sensory HCs, which convert sound vibrations into neuronal signals. Usher protein complex 1 (encoded by *MYO7A*, *USH1C*, *USH1G*, *PCDH15*, and *CDH23*) is localized at the tip links and lateral links of HC stereocilia, specialized structures that mediate mechanoelectrical transduction. Disruption of this complex compromises the physical coupling between stereocilia, leading to defective sound and balance perception. Usher protein complex 2 (encoded by *USH2A*, *ADGRV1*, *WHRN*, and *PDZD7*) is found at the ankle links, which provide structural support and maintain proper stereocilia organization. In the retina, components of Usher protein complex 1 are localized at membrane interfaces between the calyceal processes and the basolateral region of the outer segment in both rods and cones and at the junction between the inner and outer segments in rod photoreceptors. These regions are critical for maintaining the structural stability and alignment of the photoreceptor outer segments. In contrast, Usher protein complex 2 is concentrated at the periciliary region of photoreceptors, where it supports the organization and trafficking of proteins essential for photoreceptor maintenance and function.[7]

Several animal models have been used to study the underlying process of USH and to establish potential therapies.[5] Historically, mice have served as USH models, but they only partly recapitulate the retinal phenotype, which is generally milder in rodents.[5,8] This discordance with the human phenotype is attributed to mouse photoreceptors lacking human-like calyceal processes and periciliary membranes.[5] However, due to the existence of USH genes in humans which have not yet been discovered, as is evident from unsolved genomic loci, we used knockout (KO) mouse lines to search for novel candidates, despite these species differences. These candidate genes may highlight new molecular mechanisms underlying the pathobiology of USH and help identify new genotype-phenotype associations.

METHODS

• **IMPC KNOCKOUT MOUSE LINES:** The IMPC[9-15] (https://www.mousephenotype.org/) consists of 13 phenotyping centers worldwide, aiming to generate and phenotype single-gene KO mouse lines for all coding genes in the mouse genome. Phenotyping data for each line are gathered using a set of tests from the International Mouse Phenotyping Resource of Standardised Screens (IMPReSS; https://www.mousephenotype.org/impress/index).[9] All lines were generated and maintained on a C57BL/6N genetic background.[10] The technology adopted for generating each single-gene KO line was initially publicly available targeted mouse embryonic stem (ES) cells[11] and then replaced by Cas9-mediated deletion strategies in 2014.[12] For each gene, the Consortium produced and phenotyped 7 males and 7 females for most tests as defined in IMPReSS. For gene KOs affecting viability, with subviability defined as <12.5% live homozygotes (HOM) from heterozygote (HET) crosses, HET mice were phenotyped. KO and corresponding age- and sex-matched wild-type (WT) control mice were phenotyped as young adults between 9 and 16 weeks of age. At 14 weeks, hearing ability was evaluated in at least 4 mutant mice, both males and females in most cases, by analyzing auditory brainstem response (ABR) at frequencies of 6, 12, 18, 24, and 30 kHz. A click-evoked ABR was optional.[13] A complete ophthalmic examination was performed at week 15 or 16. For the primary screen of retinal traits, almost all phenotyping centers used slit lamp examination (except for Baylor College of Medicine and HMGU Helmholtz Munich) and indirect fundus examination (except for Baylor College of Medicine, HMGU Helmholtz Munich, and Institut Clinique de la Souris—PHENOMIN-ICS, which instead conducted routine optical coherence tomography [OCT] cross-sectional and funduscopic imaging) as primary screen tools. Hematoxylin and eosin staining on formalin-fixed, paraffin-embedded tissues was also used by The Cen-

ter for Phenogenomics and University of California Davis. Depending on the test and/or instrumentation used, the secondary screen studies varied across the phenotyping centers and included electroretinogram (ERG), OCT, fundus imaging, and transmission electron microscopy (TEM).[14] Phenotyping data obtained from HET or HOM mice were compared with those from WT control mice from the same center with genotypes masked to the evaluators. If the phenotypic difference was statistically significant,[15] an ontology term from the Mammalian Phenotype ontology was used to describe the phenotype.[9]

The IMPC guidelines related to housing and husbandry met the requirements of the ARRIVE guidelines,[16] the Gold Standard publication Checklist reporting Guidelines, and the Genetically Altered (GA) Passport to maintain animal welfare. All procedures complied with local, state, and national regulatory guidelines and were reviewed and approved by associated institutional animal care and use committees (IACUC), animal care committees (ACC), or equivalent.

• **NOVEL CANDIDATE GENES IDENTIFIED:** The IMPC KO mouse line[9-15] database (version 23, released on April 23, 2025) was queried for 11 retinal and 2 auditory traits. Retinal traits included abnormal retina morphology, retina pigmentation, eye electrophysiology, outer nuclear layer morphology, blood vessel morphology, vasculature morphology, blood vessel pattern, inner nuclear layer morphology, optic vesicle formation, decreased total retina thickness, and increased total retina thickness, but auditory traits were of abnormal ABR and abnormal otic vesicle morphology.

To identify potential candidate genes for USH that are not part of the 16 genes mentioned previously, the genes correlated with hearing and retina abnormality were screened for those that had at least 1 retinal and 1 auditory trait concurrently. To increase the stringency of assessing disease causation, only candidate genes causing bilateral retinopathy in most mice (a minimum of half of the KO mice affected in males and/or females) and/or were validated by histopathology were included. Mouse lines with retinal findings that did not meet these additional criteria were excluded, despite achieving statistical significance by IMPC standards.

• **SUBSTITUTION OF MOUSE GENES WITH HUMAN ORTHOLOGS:** We used the GeneCards database (https://www.genecards.org) version 5.25 (updated: July 23, 2025)[17,18] to search for human orthologues of the candidate mouse genes for multiple analyses, including protein interactions, molecular functions, and signaling pathways. Furthermore, mouse orthologues of inherited DSI genes were used to assess whether mouse lines with those genes disrupted recapitulate any DSI phenotypes. Using this database, we also screened the locus of the human orthologue of each candidate gene to see whether any were positioned in proximity to any of the previously mentioned 3 known mapped USH loci.

• **PROTEIN-PROTEIN INTERACTION NETWORK:** A protein interaction analysis was performed between the proteins encoded by USH genes, other established inherited DSI genes, ciliopathy genes, and our candidate genes using STRING-db v.12.0 released on July 26, 2023,[19] built into the Cytoscape 3.10.3 App, StringApp.[20] A confidence threshold of 0.9 was used to visualize any interaction between the proteins encoded by members of each group. To delve deeper into possible interactions among the 4 gene sets, an analysis with a confidence level of 0.7 was also performed.

• **MOLECULAR FUNCTIONS AND SIGNALING PATHWAYS:** An analysis based on v.19.0 of the PANTHER classification system, released on June 20, 2024 (https://www.pantherdb.org/), was conducted to investigate the molecular functions contributed by each gene group.[21,22] Associated signaling pathways were analyzed by KEGG, Reactome, and WIKI pathways through the Database for Annotation, Visualization, and Integrated Discovery (DAVID) knowledge base v.2025_1, released on April 17, 2025 (https://davidbioinformatics.nih.gov/).[23,24]

• **ASSESSMENT OF GENE EXPRESSION IN RETINA AND INNER EAR:** Gene expression in the retina was analyzed using the expression plot of Platform for Analysis of scEiad (single cell eye in a disk) or Plae v.0.95 (https://plae.nei.nih.gov/).[25] We used the "CellType_predict" cell grouping and set the facet on "Gene," in addition to "organism" and "CellType_predict" as filter categories in a minimum of 50 cells per group to narrow our analysis to include the data from *Homo sapiens* and *Mus musculus* separately. As RP in USH predominantly affects rod photoreceptors and/or retinal pigment epithelium (RPE) cells,[6] we checked the expression of the candidate genes and USH genes only in these cells, based on "Mean Log2(Counts+1)" values which were colored based on "study_accession." Consequently, if the presented value for RPE cells and/or rod photoreceptors was >0, then the gene was considered to be expressed in the retina. For values equal to 0, the expression was considered as not detected. Similarly, we used the Gene Expression Analysis Resource (gEAR)[26] portal v.2 (https://umgear.org/) to analyze the expression of each candidate and USH gene in the cochlea and/or vestibular HCs of humans and mice. Expression of the gene in either the cochlea or vestibular HCs was considered as the expression of the gene in the inner ear. The Human Inner Ear and Inner Ear Organoid (van der Valk and associates[27]) profile was used for detection of gene expression in humans. In this profile, single-nucleus RNA sequencing (snRNA-seq) of inner ear HCs at fetal age weeks 7.5 and 9.2 exhibits the transcription of each gene in vestibular HCs, as the mature cochlea is still in development.[27] The single-cell RNA sequencing

(scRNA-seq) data of vestibular and inner HCs/outer HCs (IHC/OHC) demo profiles were used to identify the expression of candidates in the utricle and cochlear HCs of mice, respectively.

• **ASSOCIATION WITH RETINAL DISORDERS AND DEAFNESS:** We used the retinal information network (RetNet, https://retnet.org/), accessed on September 5, 2025, to find any known association of human orthologs of candidate genes with retinopathies or mapped loci associated with retinopathies.[28] Furthermore, we carried out a similar study for hearing impairment using the Shared Harvard Inner-Ear Laboratory database (SHIELD, https://shield.hms.harvard.edu/),[29] accessed on September 5, 2025, and the Deafness Variation Database (DVD, https://deafnessvariationdatabase.org/) v.9.2, accessed on September 30, 2025.[30] In DVD, we searched through the variant table of each represented gene using the value of hearing impairment in the phenotype field. The 263 genes related to ciliopathies, a combination of Syscilia and Ciliacarta, and 39 genes of other inherited DSI illnesses were derived from Higgins and associates[31] and Guimaraes and associates,[2] respectively. In addition, previously established associations of the candidate genes with retinal, hearing, and other clinical phenotypes in humans were retrieved from Online Mendelian Inheritance in Man, OMIM. McKusick-Nathans Institute of Genetic Medicine, Johns Hopkins University (Baltimore, MD), https://omim.org/, accessed in September 2025.

• **LITERATURE REVIEW ON KO MOUSE LINES:** To investigate the retinal and auditory phenotypes of variant mouse lines in greater detail, we performed a literature search on KO and/or HET mouse lines for each candidate and mouse orthologue of inherited DSI genes, which were generated and studied for inner ear and retinal abnormalities. The auditory and retinal phenotypes of these lines were individually investigated (https://pubmed.ncbi.nlm.nih.gov/ and https://scholar.google.com/) by searching "gene symbol," "knockout," or "deletion" or "null," "mouse," "ear," "retina," "hearing," and "eye" terms to make associations between the genes and the aforementioned abnormal traits.

• **ETHICS STATEMENT:** The study was approved by the institutional review board of Partners HealthCare System and adhered to the Declaration of Helsinki. Informed consent was obtained from all individuals on whom genetic testing and further molecular evaluations were performed.

• **CLINICAL EVALUATION:** Patients and available family members from 230 families with syndromic or nonsyndromic IRD were ascertained at Massachusetts Eye and Ear and enrolled in a study assessing elusive causality. Clinical evaluation was performed by experienced ophthalmologists according to previously published protocols and included functional and structural assessment.[32–35]

• **GENETIC ANALYSIS:** Blood samples were obtained from probands and, when possible, their family members. DNA was isolated from peripheral blood lymphocytes by standard procedures. Genome sequencing (GS) was performed at Massachusetts Eye and Ear; data were aligned to hg38, and variant calling was performed using DRAGEN-GATK4 best practices. GATK-structural variant (SV) cohort mode using 5 different algorithms was used for structural variant calling.[36]

• **STATISTICAL ANALYSIS:** Statistical analysis was done using GraphPad Prism v.10.5.0. ERG data were presented as mean ± SD. Owing to the different variances among the groups (53 WT vs 4 *Mpdz*$^{-/-}$ and 3 *Rnf10*$^{-/-}$ mice), Welch's *t* test was used to compare the ERG wave amplitudes. A $P < .05$ was considered statistically significant. For OCT data, presented as mean ± SD, retinal thickness was compared between *Idua*$^{-/-}$ and WT mice using the Wilcoxon rank sum test, with significance defined as $P < .05$. The ABR test results in KO lines, conducted by IMPC, with *P* values equal to or lower than 10^{-4} ($P \leq .0001$) were marked as significant.

RESULTS

• **IDENTIFICATION OF CANDIDATE HUMAN USH GENES:** We queried KO mouse lines phenotyped by the IMPC for retinopathy and hearing abnormalities. We found 813 genes with at least 1 of 11 distinct abnormal retinal phenotypes and 338 genes with at least 1 of 2 distinct ear abnormalities. A total of 50 genes were identified that caused both auditory and retinal abnormalities in the same mouse line (Figure 1, A). Among these, 18 genes were considered high-likelihood candidates for USH because the resultant retinopathy was either confirmed by histopathology and/or was documented with bilaterally symmetric retinal abnormalities in most males and/or females of each mutant mouse line: *AA986860* (MMRRC:066881-UCD), *Adipor1* (EM:08491), *Ankrd11* (retina phenotype: EM:00380, ear phenotype: EM:07651), *Atp8b1* (MMRRC:067151-UCD), *Chsy1* (MMRRC:067396-UCD), *Cstb* (EM:09566), *Dyrk1b* (EM:10419), *Eef1d* (MMRRC:066978-UCD), *Fer* (MMRRC:066693-UCD), *Idua* (EM:15473), *Mpdz* (MMRRC:048630-UCD), *Pigq* (MMRRC:043931-UCD), *Rnf10* (retina phenotype: MMRRC:049477-UCD and MMRRC:049478-UCD, ear phenotype: MMRRC:049477-UCD), *Slc20a2* (retina phenotype: EM:08067, ear phenotype: EM:05549), *Spred1* (EM:12627), *Sun1* (EM:09532), *Tmem145* (MMRRC:065589-UCD), and *Xrcc5* (EM:12867).[9-15] Interestingly, genes such as *Ankrd11*, *Dyrk1b*, *Eef1d*, and *Slc20a2* induced relevant USH phenotypes in heterozygous individuals, whereas for the other genes, these phenotypes were only observed in homozygous mutants. The situation

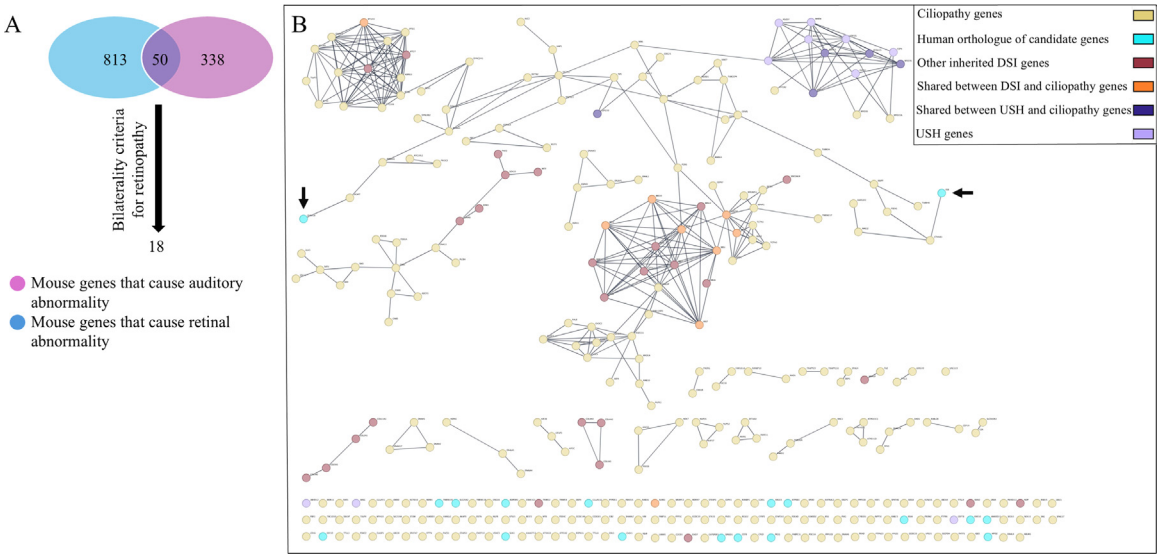


FIGURE 1. Identification of candidate gene list and protein interactions between proteins encoded by candidate genes and human Usher syndrome genes, other inherited dual sensory impairment syndrome genes, or confirmed ciliopathy genes. (A) In the Venn diagram, IMPC genes associated with retinopathy are in blue and auditory abnormality causative genes are in pink. The mutual part indicates 50 genes that result in both abnormal phenotypes, concurrently. The group of 50 was further distilled to 18 genes based on our bilaterality criteria for retinopathy. (B) STRING database was used for protein interaction analysis between proteins encoded by human orthologs of candidate genes and human USH genes, other established inherited DSI genes, or confirmed ciliopathy genes. Each of these nodes indicates an encoded protein where human USH proteins, human orthologs of candidate proteins, confirmed ciliopathy proteins, and other inherited DSI proteins are exhibited as nodes colored in lilac, blue, yellow, and red, respectively. Shared proteins encoded by the list of other inherited DSI genes and confirmed ciliopathy genes are in orange. Similarly, mutual proteins among human USH proteins and ciliopathy proteins are exhibited in purple nodes. Any interaction between the protein product of each gene with a confidence ≥0.9 is illustrated as a line. No associations between proteins encoded by human orthologs of candidate genes and human USH genes or other inherited DSI were detected. However, 2 separate interactions between the ciliopathy and candidate proteins (FER and DYRK1B, illustrated by the arrows) were detected. DSI = dual sensory impairment; USH = Usher syndrome.

for homozygous mutant genes is comparable to the AR inheritance of USH mutations, whereas the others may correspond in humans to a combination of partial loss of function. These 18 new genes, which are not part of the USH gene list, were considered candidate genes for human USH. Human orthologues for 11 of these genes (*SPRED1*, *PIGQ*, *IDUA*, *ANKRD11*, *ATP8B1*, *CHSY1*, *MPDZ*, *EEF1D*, *CSTB*, *DYRK1B*, *SLC20A2*) were associated with other clinical phenotypes in humans (Supplementary Table 1).

In addition to hearing abnormality (Supplementary Figure 1) and retinopathy, many of these 18 mutant lines had abnormalities in other physiological systems as well, resulting in an expansion of the focus of our study to other inherited forms of DSI.[2] If a particular mutant mouse line affected all the physiological systems similar to a known form of a human DSI syndrome, that gene was considered to be a candidate for the associated DSI disease. Some mouse lines reported here had significant but not complete similarity with DSI syndromes. As a result, the mutant lines that manifested phenotypes in at least 2 physiological systems in addition to visual and auditory systems were also considered positive hits for these DSI disorders, as summarized in Table 1 (all phenotyping data are available in Supplementary Data Sheet 1).

• **ACCURACY OF MOUSE LINES IN REPLICATING HUMAN DSI PHENOTYPES:** We wished to determine whether any of the 18 candidate genes had published mouse models with retinal or hearing phenotypes. Through literature search, we found that published papers from independent laboratories revealed all 6 candidate genes studied for retinopathy in KO mice (*Adipor1*,[37] *Chsy1*,[38] *Idua*,[39] *Rnf10*,[40] *Sun1*,[41] and *Xrcc5*[42]) to have retinal abnormalities and all 4 candidate genes studied for inner ear abnormalities in KO mice (*Atp8b1*,[43] *Idua*,[44] *Mpdz*,[45] and *Sun1*[46]) to have the respective abnormalities. We did not find reports of negative retinal or hearing phenotypes in any KO mouse models of the 18 candidate genes.

Furthermore, we wished to assess the degree to which mouse models of USH genes and other established inherited DSI syndromes recapitulate the spectrum of findings found in humans. To this end, we queried the literature for reports of KO mouse models of 15 human USH genes (10 confirmed genes and 5 known human candidates).[2,6] We also queried the IMPC database for any retinal and/or

TABLE 1. Candidate Genes Whose Mouse Lines Are Phenotypically Similar to Non-Usher Inherited Dual Sensory Impairment Syndromes.

Inherited Dual Sensory Impairment Syndromes	Related Candidate Genes
Bardet-Biedl syndrome	*Atp8b1, Fer, Idua, Pigq, Rnf10, Slc20a2, Spred1, Sun1, Tmem145, Xrcc5*
Alstrom disease	*Atp8b1, Fer, Pigq, Rnf10, Spred1, Sun1, Xrcc5*
Tietz albinism deafness syndrome	None found
Waardenburg syndrome	*Chsy1*
Kearns-Sayre syndrome	*Adipor1, Ankrd11, Atp8b1, Dyrk1b, Fer, Mpdz, Pigq, Rnf10, Spred1, Sun1, Tmem145, Xrcc5*
Maternally inherited diabetes and deafness	*Adipor1, Atp8b1, Fer, Mpdz, Rnf10, Spred1, Sun1, Tmem145, Xrcc5*
Stickler syndrome	*Atp8b1, Fer, Pigq, Rnf10, Spred1, Xrcc5*
Norrie disease	*Ankrd11, Atp8b1, Dyrk1b, Pigq, Rnf10, Spred1, Sun1, Tmem145*
Charge syndrome	*Adipor1, Ankrd11, Atp8b1, Cstb, Fer, Idua, Mpdz, Pigq, Rnf10, Slc20a2, Spred1, Sun1, Xrcc5*
Alport syndrome	*AA986860*, *Atp8b1*, *Eef1d*, *Fer*, *Rnf10*, *Spred1, Tmem145, Xrcc5*

Note: Mutant mouse lines of the candidate genes associated with these syndromes revealed abnormal phenotypes in at least 2 different physiological systems similar to the systems affected by the syndrome, in addition to the retina and hearing phenotype.

TABLE 2A. Comparison of IMPC Phenotyping Results and Independent Laboratory Findings Based on Our Literature Search Regarding Mutant Mice of Mouse Orthologs of Human Usher Genes.

Mouse Ortholog of Usher Syndrome Genes	IMPC Retina Findings	IMPC Inner Ear Findings	Literature Retina, PMID	Literature Retina Findings	Literature Inner Ear, PMID	Literature Inner Ear Findings
Abhd12	Not tested	Not tested	23297193	Negative	23297193	Positive
Adgrv1	Negative	Positive (abnormal ABR)	17295842	Negative	17295842	Positive
Arsg	Negative	ABR done, results not yet analyzed	26975023	Positive	22689975; 31927188	Negative
Cdh23	Eye test done, results not yet analyzed	Not tested	—	—	21436032; 20332152	Positive
Cep250	Negative	Positive (abnormal ABR)	36857066	Positive	36857066	Positive
Cep78	Negative	Negative	36206347	Positive	36206347	Positive
Clrn1	Negative	Positive (abnormal ABR)	26943149	Positive	19680541	Positive
Espn	Negative	Not tested	—	—	10975527	Positive
Myo7a	Negative	ABR done, results not yet analyzed	31824252	Positive	31824252	Positive
Pcdh15	Not tested	Not tested	12939319	Negative	18085631	Positive
Pdzd7	Not tested	Not tested	24334608	Negative	24334608	Positive
Ush1c	Negative	ABR done, results not yet analyzed	20211154	Positive	20211154	Positive
Ush1g	Not tested	Not tested	37328946	Positive	37328946	Positive
Ush2a	Not tested	Not tested	17360538	Positive	33498833	Positive
Whrn	Negative	Not tested	20502675	Positive	20502675	Positive

auditory abnormality using the same set of 15 USH genes (Table 2, A). The IMPC data included studies on the retinal phenotype in only 9 KO and/or HET mouse lines among the 15 USH genes: *Adgrv1*, *Arsg*, *Cep250*, *Cep78*, *Clrn1*, *Espn*, *Myo7a*, *Ush1c*, and *Whrn*. The other 6 genes were either not tested or not fully analyzed. The IMPC also studied the hearing phenotype in 4 KO mouse lines of the 15 USH genes: *Adgrv1*, *Cep250*, *Cep78*, and *Clrn1*. Only these 4 lines had complete phenotyping of the eye and ear. The other 11 genes were not tested for hearing, or the results of the tests were not analyzed. Of the 4 lines, 3 had abnormal ABR results. None of the 9 lines with ocular phenotyping data had retinopathy.

Analysis of peer-reviewed articles for mouse models of the same 15 human USH genes revealed that 14 of the 15 had hearing abnormalities. Only 13 of the 15 mouse models

had published evaluations of the retina, and 9 of the 13 had a retinal phenotype, but 4 of the 13 had a normal retina.

To compare IMPC screening to independent laboratories in a head-to-head comparison, we found just 4 genes that had retinal and hearing evaluations reported by both screening paradigms. Four genes (*Adgrv1*, *Cep250*, *Cep78*, and *Clrn1*) had mouse models studied for both retinal and inner ear phenotypes by independent laboratories, revealing concurrent retina and inner ear abnormalities in 3 of 4 lines (*Cep250*, *Cep78*, and *Clrn1*). The IMPC screening of these 4 lines revealed no retinopathy in any of them but ear abnormalities in 3 of 4 (*Adgrv1*, *Cep250*, *Clrn1*). The results suggest that longitudinal study of mouse models of USH (as in the published literature) is more sensitive than the high-throughput snapshot screening used by the IMPC. We also concluded that mouse models of USH, when studied longitudinally, recapitulate the human findings associated with hearing (14/15, 93.3%), but the retinal abnormalities were not modeled as faithfully (9/13, 69.2%). All data are found in Table 2, A.

A similar analysis was performed on mouse lines for the other (non-USH) inherited DSI-confirmed genes (Table 2, B). There were 39 known DSI genes exclusive of USH.[2] The IMPC has generated and phenotyped the retina of KO/HET/hemizygous mice for 22 of 39 confirmed DSI genes: *Alms1*, *Bbip1*, *Bbs1*, *Bbs4*, *Bbs5*, *Bbs7*, *Bbs9*, *Bbs10*, *Bbs12*, *Cep290*, *Cfap418*, *Chd7*, *Col11a1*, *Col2a1*, *Col4a3*, *Col4a4*, *Col4a5*, *Col9a2*, *Ift172*, *Ift74*, *Mks1*, and *Snai2*. Two of these 22 lines had retinal phenotypes (*Bbs5* and *Ift72*, 9.1%). The IMPC has also reported on the hearing ability of 14 KO/HET/hemizygous mouse lines of the 39 DSI genes: *Alms1*, *Bbs1*, *Bbs4*, *Bbs7*, *Bbs10*, *Cep290*, *Cfap418*, *Col4a3*, *Col4a4*, *Col4a5*, *Col9a2*, *Ift172*, *Ift74*, and *Snai2*. Only *Col9a2* (1/14, 7.1%) had abnormal hearing.

Independent publications evaluated mouse models for 20 of 39 DSI genes for retinal abnormalities and found phenotypes in 17 of them (17/20, 85%). Independent laboratories evaluated hearing for 16 DSI genes using mouse models, all of which were abnormal (16/16, 100%).

We then performed a head-to-head comparison of DSI mouse models between IMPC high-throughput snapshot screening and longitudinal evaluation by independent research laboratories. Furthermore, 11 lines were analyzed by both paradigms for retinal phenotypes, and 6 lines were analyzed by both methods for hearing. Only 2 lines were characterized for both inner ear and retinal phenotypes by both strategies. The results are outlined in Table 3.

Taken together, these data suggest that mouse models of USH and other DSI syndromes recapitulate human findings when studied longitudinally, as in the case of peer-reviewed articles from independent research laboratories. However, the IMPC high-throughput phenotyping pipeline was relatively less sensitive (but specific) in picking up these abnormalities. This could be due to the nature of high-throughput screening, so that only the most prominent phenotypes are recorded. In contrast, individual research projects looking at specific genes are more focused and conduct deeper phenotyping.

• **ANALYZING THE EXPRESSION OF USHER GENES AND CANDIDATE GENES IN THE RETINA AND INNER EAR:** A total of 15 human USH genes and 18 candidate genes were analyzed for retinal expression (in rods and/or RPE cells) and in inner ear cells (cochlear and/or vestibular HCs) in humans and mice, cells that are primarily affected in RP and/or SNHL, as found in USH.[6]

We screened the Plae database[25] to study the expression of the 2 gene sets in the rods and/or RPE cells of the retina of both species. We found that 13 of 15 human USH genes (86.6%) are expressed in the retina of humans and mice. The expression of *CLRN1* and *USH1G* was not detected in human rods and/or RPE cells. Mouse rods and/or RPE cells had no transcripts of *Ush1g* and *Pdzd7*. In terms of our candidate genes, 16 of 18 (88.8%) and 17 of 18 (94.4%) are expressed in the retina of humans and mice, respectively. No expression of *ATP8B1* and *C1orf116*, the human orthologue of the candidate gene *AA986860*, was reported in rod photoreceptors or RPE cells of the human retina, and no transcripts of *Atp8b1* were identified in mouse rods and/or RPE cells (Supplementary Figure 2). The lack of gene expression reported by the Plae database may be because of the low expression of the gene of interest, which could not be detected by scRNA-seq analysis, or because there is no expression at all. Furthermore, an investigation through the gEAR[26] database revealed the expression of all candidate genes and human USH genes in the inner ear HCs of both mice and humans (18/18 candidate genes, 15/15 USH genes) (Supplementary Figures 3-8).

• **PROTEIN INTERACTION ANALYSIS:** We sought to predict whether any protein encoded by the 18 human orthologues of candidate genes interacts with any encoded protein among the 15 human USH genes, the 39 genes associated with other inherited DSI syndromes derived from Guimaraes and associates,[2] or the 263 known ciliopathy genes, a combination of Syscilia and Ciliacarta, from Higgins and associates.[31] *MT-TL1* from other inherited DSI (a causative mitochondrial gene of maternally inherited diabetes and deafness, coding for a leucine tRNA[47]) and *PTCHD3*, from ciliopathy genes, are not represented in the STRING-db[19,20] and thus could not be analyzed.

No known protein-protein interaction between the 18 candidates and 15 human USH genes or between the 18 candidates and the other 38 inherited DSI genes was found (Figure 1, B). Notably, we found that FER and DYRK1B, both from our list of 18 candidates, interact with CTNNB and DCAF from the ciliopathy list, respectively. To further explore the protein-protein interactions present between the candidates and other gene collections, the confidence level was reduced to 0.7. With this confidence level, 3 new interactions were noted between protein products of *CSTB*, *SPRED1*, and *XRCC5* of candidate genes with *TRAPPC10*,

TABLE 2B. Comparison of IMPC Phenotyping Results and Independent Laboratory Findings Based on Our Literature Search Regarding Mutant Mice of Mouse Orthologs of Non-Usher Inherited Dual Sensory Impairment Syndrome Genes.

Mouse Ortholog of Inherited Dual Sensory Impairment Syndrome Genes	IMPC Retina Findings	IMPC Inner Ear Findings	Literature Retina, PMID	Literature Retina Findings	Literature Inner Ear, PMID	Literature Inner Ear Findings
Alms1	Negative	Negative	16000322	Positive	16000322	Positive
Arl6	Not tested	Not tested	22139371	Positive	—	—
Bbip1	Negative	ABR done, results not yet analyzed	—	—	—	—
Bbs1	Negative	Negative	—	—	16170314	Positive
Bbs10	Negative	Negative	36125046	Positive	—	—
Bbs12	Negative	ABR done, results not yet analyzed	22869374	Positive	—	—
Bbs2	Not tested	Not tested	15539463	Positive	—	—
Bbs4	Negative	Negative	15173597; 29049287	Positive	19396898	Positive
Bbs5	Positive (abnormal retina morphology)	Not tested	32776140	Positive	—	—
Bbs7	Negative	Negative	23572516	Positive	—	—
Bbs9	Negative	Not tested	—	—	—	—
Cep290	Negative	Negative	25859007	Positive	—	—
Cfap418	Negative	Negative	29440555; 37971880	Positive	—	—
Chd7	Negative	Not tested	26670829	Positive	34004180	Positive
Col11a1	Negative	Not tested	—	—	22567353	Positive
Col2a1	Negative	ABR done, results not yet analyzed	16546167	Negative	—	—
Col4a3	Negative	Negative	—	—	9682811	Positive
Col4a4	Negative	Negative	—	—	21196518	Positive
Col4a5	Negative	Negative	—	—	—	—
Col9a1	Not tested	Not tested	16909383	Negative	15802199	Positive
Col9a2	Negative	Positive (abnormal ABR)	—	—	31161720	Positive
edn3	Not tested	Not tested	8001160	Negative	—	—
Ednrb	Not tested	Not tested	—	—	21715336	Positive
Ift172	Positive (abnormal retina blood vessel morphology)	Negative	29659833	Positive	—	—
Ift27	Not tested	Not tested	—	—	25605782	Positive
Ift74	Negative	Negative	—	—	—	—
Lztfl1	Not tested	Not tested	27312011	Positive	—	—
Mitf	Not tested	Not tested	31659211	Positive	31659211	Positive
Mkks	Not tested	Not tested	22446187	Positive	22446187	Positive
Mks1	Negative	Not tested	—	—	—	—
mt-Tl1	—	—	—	—	—	—
Ndp	Not tested	Not tested	12040033; 8789439	Positive	34544869	Positive
Pax3	Not tested	Not tested	—	—	38278860	Positive
Sdccag8	Not tested	Not tested	—	—	—	—
Snai2	Negative	Negative	—	—	—	—
Sox10	Not tested	Not tested	—	—	—	—
Trim32	Not tested	Not tested	—	—	—	—
Ttc8	Not tested	Not tested	29049287	Positive	25605782	Positive
Wdpcp	Not tested	Not tested	—	—	—	—

ABR = abnormal auditory brainstem response; IMPC = International Mouse Phenotyping Consortium; PMID = PubMed identifier.

Note: The results revealed that the longitudinal studies conducted by independent laboratories may be more successful in identifying abnormal phenotypes of mutant mouse lines of Usher syndrome genes (A) and other inherited dual sensory impairment syndrome genes (B) compared with the high-throughput "snapshot-in-time" screening done by IMPC centers.

TABLE 3. Comparing the Head-to-Head Concordance of Retinal and Auditory Phenotypes Between Similar Mutant Mouse Lines From the IMPC and Peer-Reviewed Articles From Independent Researchers.

Phenotype in Knockout Mouse Models	IMPC Knockout Mouse Lines	Peer-Reviewed Articles of Knockout Mouse Lines
Retinal abnormality	USH: 0/9	USH: 7/8
	Other inherited DSI: 2/22	Other inherited DSI: 10/11
Hearing abnormality	USH: 3/4	USH: 4/4
	Other inherited DSI: 1/14	Other inherited DSI: 6/6
Mouse models with both phenotypes evaluated	USH: 0/4	USH: 3/4
	Other inherited DSI: 0/14	Other inherited DSI: 2/2

DSI = dual sensory impairment; Het = heterozygous; IMPC = International Mouse Phenotyping Consortium; KO = knockout; USH = Usher syndrome.

Note: Of the 15 USH genes in humans, each has a mouse orthologues. Of these 15 mouse genes, the IMPC has phenotyped the retina of 9 and the hearing ability of 4 KO/HET lines. Independent laboratories in the peer-reviewed literature evaluated reported retinal abnormalities in 8 of the 9 genes, and hearing abnormalities in all 4 lines. The IMPC phenotyping process found 0 of 9 or 3 of 4 of the mouse orthologues of human USH genes have retinopathy or hearing impairment, respectively. Of these 4 lines studied by independent laboratories, all had a definitive hearing impairment, and of the 8 KO lines that underwent ophthalmologic assessment, 7 exhibited retinal abnormality. Furthermore, independent studies revealed that among 4 IMPC KO lines, which were phenotyped regarding both retina and inner ear, 3 exhibited abnormalities concurrently. However, these abnormalities were not reported by IMPC (0/4). Similarly, of the 39 other DSI genes in humans, all have a mouse orthologues. Of these 39 genes, the IMPC had phenotyped the retina of 22 and hearing ability of 14 KO/HET/hemizygous lines. The IMPC data revealed that 2 of 22 (9.1%, *Bbs5* and *Ift172*) of these models had retinopathy. In addition, 1 of 14 (7.1%, *Col9a2*) mutant lines have hearing impairment. Only 11 of these 22 genes and 6 of these 14 genes with IMPC mutants have mouse lines evaluated by independent laboratories in the peer-reviewed literature for head-to-head comparison regarding retina and inner ear, respectively. In the published literature, 10 lines documented evidence of retinopathy, and all 6 lines had abnormalities in the inner ear. In addition, of 14 IMPC mutant lines, which were studied for both retinopathy and inner ear abnormality, only 2 were studied regarding both retina and inner ear by the independent laboratories. Both lines (*Bbs4* and *Alms1*) had abnormal phenotypes simultaneously. Although IMPC phenotyping is comprehensive for all systems, some of these lines generated by others were not evaluated for all systems. Mutant mouse models of bona fide human USH/DSI genes relatively faithfully recapitulate both hearing and retinal abnormalities found in people, but longitudinal screening may be required to identify them, whereas high-throughput snapshot screening may miss subtle defects, especially on the *rd8* background.

RAF1, and *ORC1* of ciliopathy genes, respectively (Supplementary Figure 9).

• **MOLECULAR FUNCTIONS AND SIGNALING PATHWAYS ANALYSIS:** We used bioinformatic tools to identify relationships between the molecular functions and signaling pathways in our candidate gene set and sets of human USH and other established DSI genes. The PANTHER classification system[21,22] reveals the existence of 3 similar molecular functions shared among our candidate genes, the human USH genes, and other inherited DSI genes: ATP-dependent activity, binding, and catalytic activity. Molecular function regulator and molecular transducer activities are shared only between the gene profiles of candidates and other inherited DSI genes. Furthermore, each gene set was found to have unique molecular functions. Candidate genes (Figure 2, Left) were uniquely associated with molecular adaptor and transporter activities, but only human USH genes were associated with cytoskeletal motor activity (Figure 2, Middle). In addition, other (non-USH) inherited DSI syndrome genes uniquely participated in structural molecule and transcription regulator activities (Figure 2, Right).

We used DAVID[23,24] to study the related pathways in which the candidate genes and the 2 other gene sets are involved. Three different signaling pathway databases were studied using this bioinformatic tool: KEGG, Reactome, and WIKI pathways. KEGG revealed that candidate genes shared the lysosome pathway with human USH genes, whereas the adherens junction and cytoskeleton in muscle cell pathway were shared by the candidate gene set and inherited DSI genes. WIKI pathways revealed no additional signaling pathway similarities (Supplementary Data Sheet 1).

According to Reactome, 4 pathways were common among the 3 gene sets: metabolism of proteins, signal transduction, post-translational protein modification, and cell cycle. Moreover, the metabolism pathway was linked to both the candidate genes and human USH genes, whereas the candidate and inherited DSI genes shared the immune system, innate immune system, neutrophil degranulation, signaling by receptor tyrosine kinases, and cytosolic sensors of pathogen-associated DNA pathways (Table 4).

MT-TL1, an inherited DSI gene, was not represented in the DAVID and PANTHER databases and thus could not be analyzed.

• **CORRESPONDENCE OF CANDIDATE GENES WITH UNSOLVED HUMAN USH LOCI:** So far, 3 human USH loci of unidentified genes, evident from mapping linkage, have

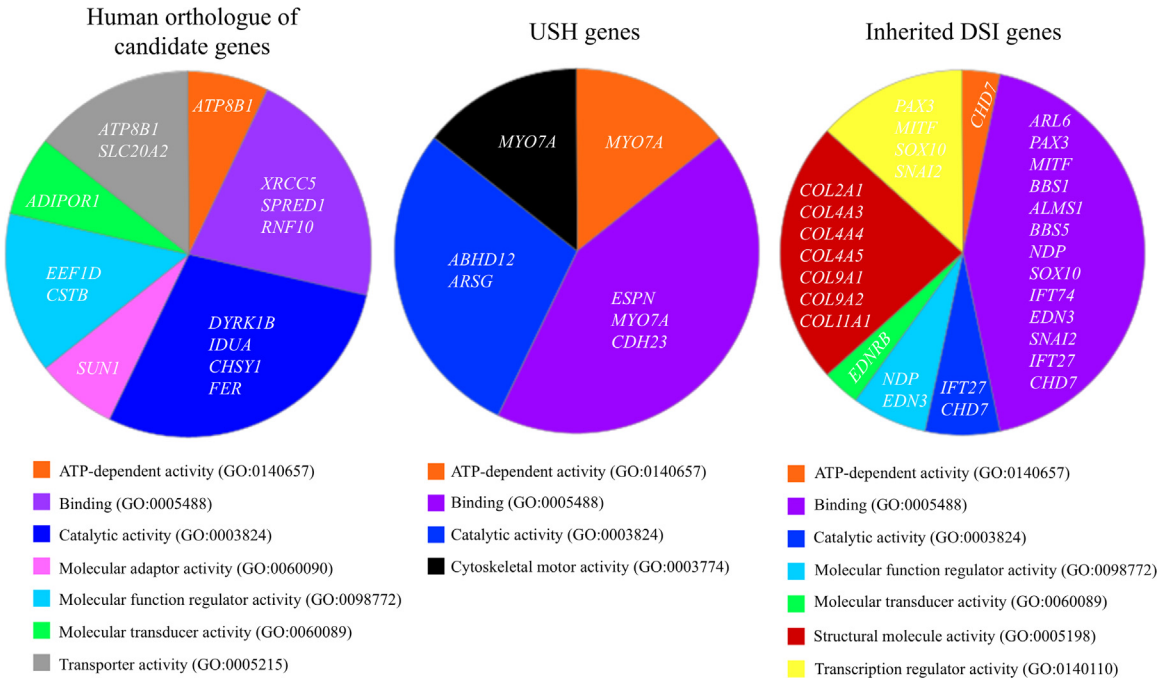


FIGURE 2. The molecular functions of the human orthologs of candidate genes (left), Usher syndrome genes (middle), and confirmed inherited dual sensory impairment syndrome genes (right), based on PANTHER V19.0 analysis. ATP-dependent activity, binding and catalytic activity overlap between 3 categories. DSI = dual sensory impairment; USH = Usher syndrome.

TABLE 4. Shared Signaling Pathways of Candidate Genes With Usher Syndrome Genes and Other Inherited Dual Sensory Impairment Syndrome Genes Based on DAVID v2025_1 Database.

Mutual Signaling Pathways Between Candidate Genes and Usher Syndrome Genes		Mutual Signaling Pathways Between Candidate and Other Inherited Dual Sensory Impairment Syndrome Genes	
KEGG	Reactome	KEGG	Reactome
Lysosome	Metabolism of proteins Signal transduction Post-translational protein modification Cell cycle Metabolism	Adherens junction Cytoskeleton in muscle cells	Metabolism of proteins Signal transduction Post-translational protein modification Cell cycle Immune system Innate immune system Neutrophil degranulation Signaling by receptor tyrosine kinases Cytosolic sensors of pathogen-associated DNA

been associated with USH1.[2,6] These loci are 10p11.21 to q21.1, 15q22 to q23, and 21q21. An analysis using the GeneCards database[17,18] revealed that 3 human orthologues of our candidate genes are adjacent to these loci: *SPRED1* at 15q14, *CHSY1* at 15q26.3, and *CSTB* at 21q22.3. Future work is needed to determine whether these candidates are related to USH1.

• **ASSOCIATION OF CANDIDATE GENES WITH RETINOPATHY OR DEAFNESS:** To further validate our candidate genes, we screened RetNet,[28] SHIELD,[29] and DVD[30] to identify any association between our candidate genes and inherited retinal diseases (IRDs) and/or deafness in human populations.

Among human orthologues of our candidate gene set, *ATP8B1* is within the CORD1 locus, *MPDZ* can cause AR macular degeneration, and *ADIPOR1* is known to cause recessive syndromic retinopathy as part of BBS, autosomal dominant (AD) RP, and syndromic or systemic diseases with retinopathy (AR).

In terms of hearing disability, pathogenic variants in *IDUA* were associated with hearing impairment in a patient with Hurler-Scheie syndrome.[48] *RNF10* is within the mapped loci of DFNA25 and DFNA41. In addition,

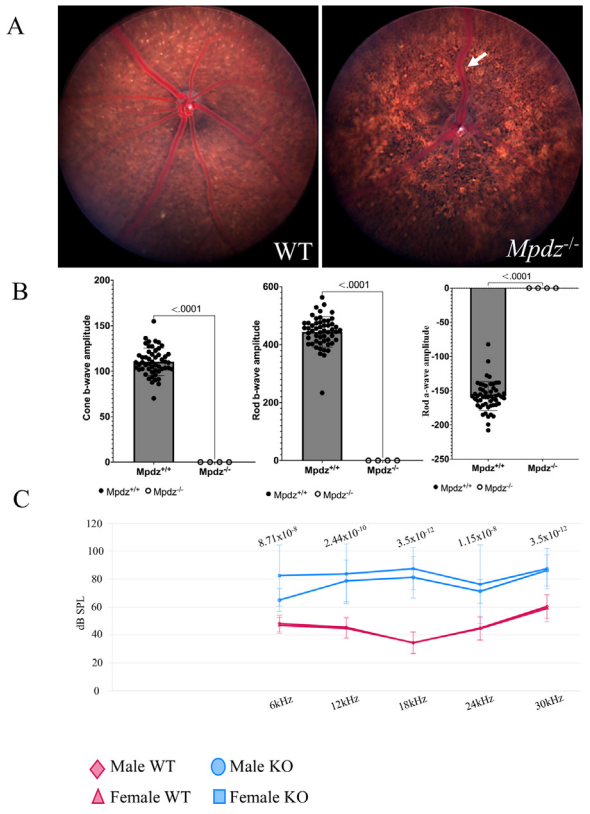


FIGURE 3. Fundus imaging, electroretinogram, and auditory brainstem response tests revealed retinal and hearing abnormalities in *Mpdz* knockout mice. (A) Fundus imaging of 14-week-old WT (left) and *Mpdz*$^{-/-}$ (right) mouse revealed abnormal retina vasculature morphology in the KO mouse (indicated by an arrow). (B) ERG on 53 WT and four *Mpdz*$^{-/-}$ mice revealed significant reduction in cone b-wave, rod b-wave, and rod a-wave amplitudes of *Mpdz*$^{-/-}$ mice ($P < .0001$). (C) Compared with the WT mice (red lines), *Mpdz*$^{-/-}$ mice (blue lines) had significantly increased ABR thresholds for all tested frequencies, indicating hearing difficulties. For each tested frequency, *P* value was generated by combining the ABR values of males ($n = 4$ KO, 591 WT) and females ($n = 4$ KO and 606 WT) of the same group. ABR = auditory brainstem response; dB SPL = decibel sound pressure level; ERG = electroretinogram; KO = knockout; WT = wild type.

CHSY1 is associated with both the DFNA30 and OTSC1 loci. Furthermore, missense variants of *CHSY1* may be causative of hearing impairment.[49]

• **MPDZ KO MOUSE MODEL, ONE OF THE CANDIDATE GENES FOR INHERITED DSI SYNDROMES:** Based on the IMPC database, the *Mpdz*$^{-/-}$ mice had abnormal retina morphology, defined by a structural anomaly of the neural retina, along with abnormal retinal blood vessels and vasculature morphology, compared with the WT mice (Figure 3 A). In addition, ERG recordings revealed a significant reduction in cone b-wave, rod b-wave, and rod a-wave amplitudes ($P < .0001$, Figure 3, B). ABR test results (Figure 3, C), conducted by the IMPC, revealed that mutant mice were associated with reduced hearing, evident by an increased ABR threshold. The increase in ABR threshold is evident across all frequencies tested (6-30 kHz). The KO was tested in the early adult stage of life. Retinal transcriptomic data from the Plae[25] database illustrate the expression of this gene in both human and mouse retina (Supplementary Figure 2), specifically in rod photoreceptors and/or RPE cells. The expression of *Mpdz* in the mouse and human inner ear HCs (Supplementary Figures 4, 7, and 8) is demonstrated by the gEAR database.[26]

According to the IMPC database, mice lacking *Mpdz* exhibit abnormalities in other physiological systems: homeostasis/metabolism (improved glucose tolerance, increased circulating potassium level), behavior/neurological (decreased grip strength, decreased startle reflex), growth/size/body region, and cardiovascular system (increased heart weight). As Charge syndrome symptoms include hearing loss, retinal and macula coloboma, retarded growth/development, and heart disease,[2] the *Mpdz* KO mouse could be a model for this syndrome. Similarly, this gene can be considered as a possible candidate for Kearns-Sayre syndrome and maternally inherited diabetes and deafness due to the cardiac and behavior/neurological abnormalities found in *Mpdz*$^{-/-}$ mouse line. Although the abnormal phenotypes resulting from loss of this gene do not exactly phenocopy Charge, Kearns-Sayre syndrome, and maternally inherited diabetes and deafness syndromes, they share significant similarities, which suggests a potential link with them.

• **IMPC HISTOPATHOLOGY:** The IMPC histopathologic analysis of the retina in a subset of the lines associated with the candidate genes revealed definite abnormalities consistent with the clinical phenotyping findings. A comparison of the retina in the WT and *Idua*$^{-/-}$ mice revealed reduced thickness in the outer nuclear layer and retina of *Idua*$^{-/-}$ mice (Figure 4, A-C). Similarly, compared with WT, severe outer retinal atrophy, including the outer nuclear layer where rod nuclei are located, was detected in *Chsy1*$^{-/-}$ mice (Figure 4, D and E). However, not all IMPC in vivo testing is corroborated by histopathology. For example, the comparison between WT and *Chsy1*$^{-/-}$ organ of Corti revealed no obvious abnormality by routine histopathology (Figure 4, F and G) despite abnormal ABR test results (Supplementary Figure 1). Retinal lamination defects were observed in the outer retina of *Fer*$^{-/-}$ and *Fer*$^{+/-}$ mice, but they were interpreted to be more likely due to the *rd8* mutation present in C57BL/6N mice, the background used by the IMPC[50] (Supplementary Figure 10, A-C). However, color fundus imaging of *Fer*-mutant mice revealed abnormal lesions that were different from the *rd8* phenotype (Supplementary Figure 11, A-C). Similarly, the retina and inner ear of *Eef1d*$^{+/-}$ mice had no obvious histopathologic abnormality (Supplementary Figure 10, D-F), despite having signs of abnormal retinal morphology on slit lamp and ophthalmoscope ex-

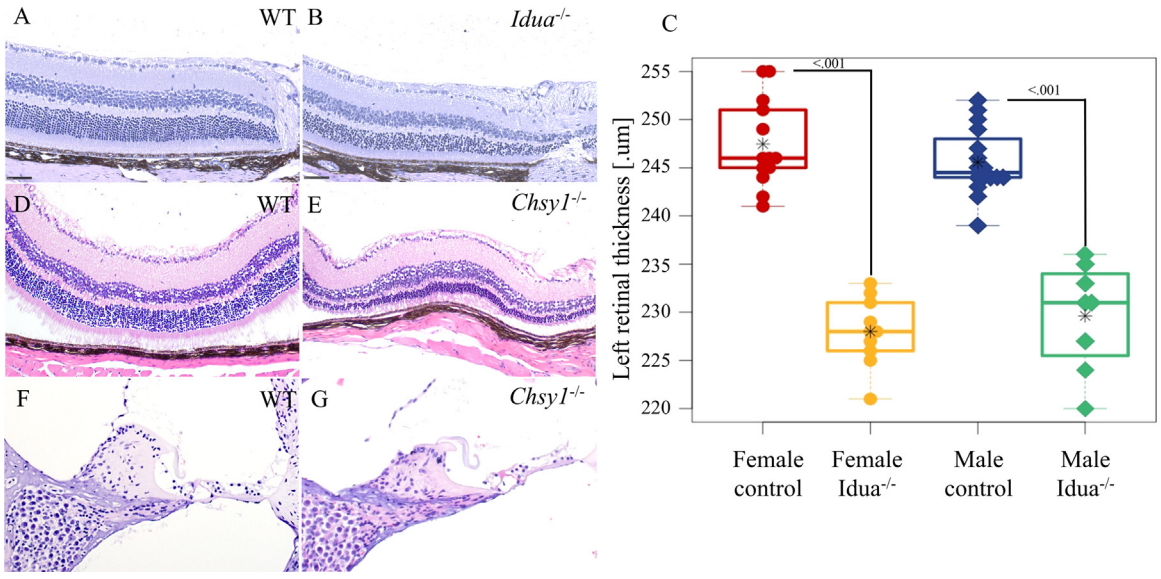


FIGURE 4. Morphologic alterations in *Idua*$^{-/-}$ and *Chsy1*$^{-/-}$ mice. Comparison of representative histologic images of mouse retinal tissue between 15-week-old WT (A) and *Idua*$^{-/-}$ mice (B) revealed a reduction in total retinal thickness and thinning of the outer nuclear layer in the KO mouse (hematoxylin and eosin). (C) Optical coherence tomography analysis comparing retinal thickness in 18 *Idua*$^{-/-}$ mice (10 females and 8 males) vs 29 WT controls (13 females and 16 males) revealed a significant reduction in retinal thickness in the first group (data are in mean ± SEM; female $P < .001$, male $P < .001$, C). Comparison of 15-week-old WT (D) and *Chsy1*$^{-/-}$ mice (E) demonstrated outer retinal atrophy in the KO line (hematoxylin and eosin). Examination of the organ of Corti in WT (F) and *Chsy1*$^{-/-}$ mice (G) revealed no detectable abnormalities (hematoxylin and eosin). KO = knockout; WT = wild type.

aminations with an abnormal ABR test result, as reported by IMPC. Although there is no available retinal or inner ear histopathology imaging of *Xrcc5*, *Spred1*, and *Rnf10* KO mice, fundus images revealed an abnormal retinal blood vessel pattern in all 3 lines, with retinal degeneration found only in *Xrcc5* and *Spred1* KO mice (Supplementary Figure 11, D-H). Comparison of ERG studies on WT and *Rnf10*$^{-/-}$ mice revealed that the amplitude of the rod a-wave and rod b-wave is significantly reduced in *Rnf10*$^{-/-}$ mice (Supplementary Figure 11, I, $P = .0278$, and Supplementary Figure 11, J, $P < .0001$).

• **SCLT1 KO MOUSE, AS A MODEL OF BBS:** BBS is a DSI syndrome and ciliopathy, similar to USH, which manifests as retinal degeneration, hearing difficulty, renal dysfunction, obesity, hypogonadism, postaxial polydactyly, and cognitive impairment, typically with an AR inheritance.[2] During our screening of IMPC KO mouse lines,[9-15] we noticed that knocking out *Sclt1*, a putative ciliopathy gene,[31] led to posterior synechiae, retinal degeneration, polycystic kidney, and polydactyly (Figure 5), confirmed by histopathology. In addition, the gEAR database reported the expression of this gene in the inner ear HCs of both humans and mice.[26]

According to DAVID/Reactome, the signaling pathways to which *SCLT1* contributes are cilium assembly, anchoring of the basal body to the plasma membrane, and organelle biogenesis and maintenance. These pathways are similar to the signaling pathways of confirmed BBS causative genes.[2,23,24]

Sclt1 homozygous KOs (HOM) are subviable, with fewer than 12.5% of HOM surviving to genotyping age, and all HOM mice died or were euthanized approximately 3 weeks of age. Only histology/histopathology studies were done on KO mice. The results of examinations of HET mice for retinal and hearing phenotypes were not significant, consistent with an AR mode of inheritance observed in BBS. Furthermore, in a previously published study done by Morisada and associates,[51] identical compound heterozygous *SCLT1* mutation was reported in 2 unrelated patients with a clinical diagnosis of BBS.[51] Therefore, *Sclt1*-mutant mice might be a good model for BBS due to phenotyping similarities with this syndrome. It would be informative to test a patient-specific variant on this background using a conditional model and/or this allele in a different strain background to determine whether the mice live long enough to undergo in-life phenotyping.

• ***SLC20A2* IS A CANDIDATE GENE FOR USHER SYNDROME:** GS in 230 unsolved IRD cases identified 1 USH proband (OGI767_1502) with a heterozygous rare variant (c.215A>C; p.Lys72Thr) in exon 2 of the Solute Carrier Family 20 Member 2 (*SLC20A2*) gene, a human orthologue of 1 of the 18 mouse candidate genes, which en-

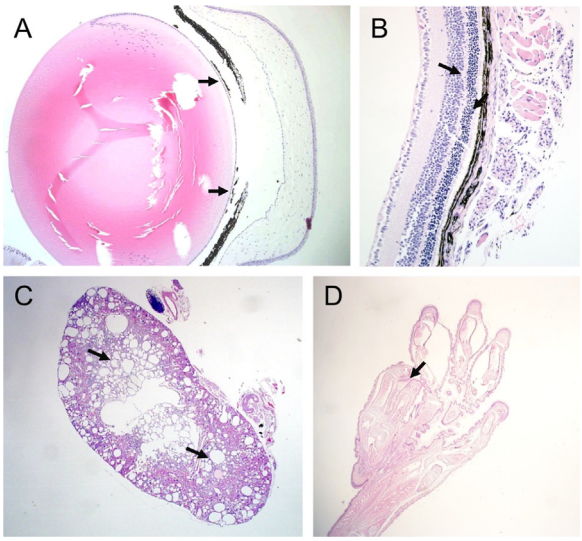


FIGURE 5. ***Sclt1*$^{-/-}$ mice had eye, kidney, and skeletal abnormalities consistent with ciliopathy. (A) Eye section, revealing posterior synechia of the iris to lens (indicated by arrows). (B) Retinal histology revealing retinal atrophy in the outer nuclear layer and outer plexiform layer (indicated by arrows). (C) Kidney section revealing multiple dilated tubules forming cystic structures, granular eosinophilic material (probably protein), and red blood cells, is evident (indicated by arrows). (D) Section of the hind paw revealing 2 first phalanges (indicated by an arrow) (hematoxylin and eosin).**

codes a member of the inorganic phosphate transporter family (Figure 6, A). Variants in this gene have been previously associated with dominant primary familial brain calcification (also known as Fahr's syndrome, OMIM 213600), which manifests with parkinsonism.[52] Sanger sequencing confirmed the presence of the p.Lys72Thr variant in the proband and excluded it from his unaffected mother and maternal half-sister (Figure 6, A). However, as DNA from the reportedly unaffected father was not available, we could neither confirm de novo inheritance nor autosomal dominant inheritance with incomplete penetrance. A known pathogenic heterozygous variant (c.5237G>A; p.Arg1746Gln) in *CDH23*, a gene associated with recessive USH type 1, was also identified on panel-based testing and confirmed on GS, but no second allele was found. Likewise, pathogenic variants in other USH-associated genes were excluded.

The *SLC20A2* c.215A>C; p.Lys72Thr missense variant was absent from the GnomAD v.4 population database (https://gnomad.broadinstitute.org),[53] as well as the LOVD[54] and ClinVar[55] databases, both of which contain curated patient variant data. The p.Lys72Thr variant was predicted to be likely causal by several in silico predictors (CADD score: 24.9; REVEL: 0.809; AlphaMissense: 0.644; MetaDome Mutation Intolerance: 0.21) but not by SpliceAI (score = 0), suggesting that the underlying pathogenic mechanism is unlikely to affect splicing. Furthermore, using ChimeraX to model the p. Lys72Thr change on the AlphaFold-predicted structure of the SLC20A2 protein, we observed that the introduced threonine at residue 72 is predicted to disrupt a hydrogen bond with the glutamine residue at position 528 and generate an additional hydrogen bond with the glutamic acid residue at position 68, thus suggesting a change in protein folding (Figure 6, B).

OGI767_1502 is a 66-year-old man diagnosed with having USH type 1 secondary to profound congenital sensorineural hearing impairment and RP. He was initially diagnosed with having RP at age 19 years with complaints of decreased night and peripheral vision loss at that time. At age 20 years, his corrected visual acuity was 20/30 in the right eye (OD) and 20/30 in the left eye (OS) with fundus findings typical of RP. Full-field electroretinography at age 20 years revealed near-nondetectable responses to scotopic bright flash and nondetectable responses to the 30 Hz stimulus. Goldmann perimetry at age 21 years was reported to reveal constriction in each eye to 10–15°and 15–20° to the I4e and V4e targets, respectively. ERG was later repeated with bandpass filtering and signal averaging to enable detection of 30 Hz responses: at age 35 years, responses were 1.4 uV OD and 1.6 uV OS with prolonged implicit times, but at age 56 years, responses had decreased to 0.68 uV OD and 0.91 uV OS.

At age 66 years, visual acuity had decreased to 20/100 OD and 20/200 OS, with dry eye and cataract also being contributory factors. Fundus examination continued to reveal typical features of RP (Figure 6, C), whereas fundus autofluorescence (FAF) OD revealed preserved FAF in the central macula but diffuse reduction and absence of FAF in the peripheral macula extending through the visible periphery (Figure 6, D). Goldmann perimetry using the I4e and V4e targets revealed generalized constriction of 10° and 20°, respectively. Optical coherence tomography OD revealed outer retinal bands, including the ellipsoid zone, present centrally but attenuated in the peripheral macula. Cystoid macular edema was also present and was treated with acetazolamide. His medical history also included learning disability and Parkinson's disease, with the latter diagnosed after age 60 years. As variants in *SLC20A2* are known to cause the parkinsonism found in Fahr's syndrome, the novel c.215A>C; p.Lys72Thr may underlie the patient's neurologic condition and may also lead to the USH1 symptoms, though with the current genetic evidence, it is classified as a variant of uncertain significance.

DISCUSSION

By analyzing different mutant mouse lines, we aimed to identify novel DSI-associated candidate genes, their

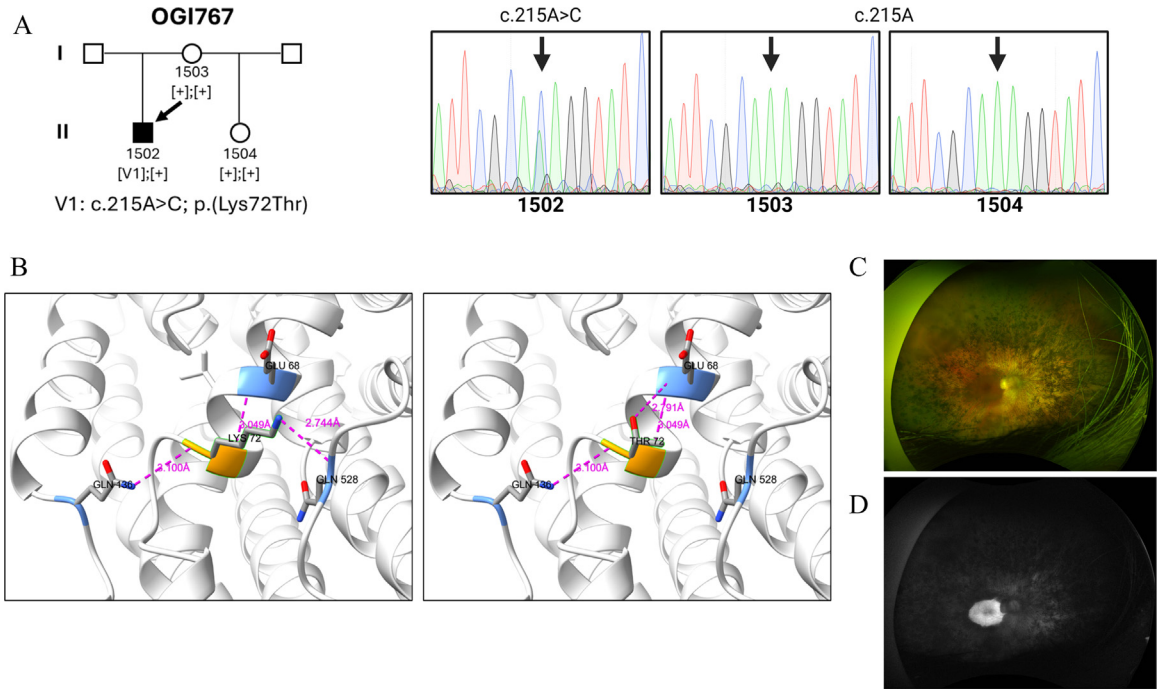


FIGURE 6. *SLC20A2* is a candidate gene for Usher syndrome. (A) Pedigree of an Usher syndrome type 1 family in which the affected proband (1502) harbors the missense variant p.(Lys72Thr) in *SLC20A2*, which is not present in the unaffected mother (1503) and maternal half-sister (1504). (B) ChimeraX-generated model of native (left) and mutated (right) SLC20A2 protein. The p.Lys72Thr is predicted to alter the hydrogen bonds (indicated by purple dotted lines) with residues of Glutamic acid (Glu) and Glutamine (Gln) at positions 68 and 528, respectively. (C) Fundus and (D) fundus autofluorescence pictures of the affected proband revealing findings typical of retinitis pigmentosa.

molecular functions, and signaling pathways. Our goal was to provide justification for research to determine disease causality, expand the genetic diagnosis in currently unsolved patients, and identify novel genotype-phenotype associations.

We found 18 novel candidate genes associated with hearing and retinal phenotypes in mouse KO lines. All these lines also demonstrated effects on other physiological systems, expanding the scope of our study to other causes of inherited DSI beyond USH. The abnormal constellation of phenotypes manifested in different physiological systems does not fully overlap with human disease owing to species-specific differences and the "snapshot-in-time" approach of the IMPC phenotyping pipeline. It is also possible that human patients may not undergo as comprehensive systemic phenotyping as mouse models. Human mutations may also be hypomorphic or neomorphic rather than loss-of-function alleles in mouse knockouts, because the latter are targeted deletions predicted to lack all gene function. Furthermore, inherited DSI syndromes are relatively uncommon in humans and may not yet be fully characterized. For instance, there have been reports of bronchiectasis, somatosensory deficit, reduced sperm motility, and olfactory loss in patients with USH.[5] Therefore, our candidate gene set could be considered for both USH and other inherited DSI syndromes. Finally, the OMIM database has reported on 11 of 18 candidate genes that were identified to have a known association with other non-sensory phenotypes, mostly neurodevelopmental disorders (Supplementary Table 1), 6 of which are reported to impair vision and/or hearing in a subset of patients. Ophthalmic involvement in *PIGQ* patients includes vertical nystagmus, hyperopia, astigmatism, and cortical visual impairment; *IDUA* mutation led to retinal degeneration, which often occurs in mucopolysaccharidosis type I, and hearing impairment in a Hurler-Scheie syndrome patient; *ANKRD11* and *CHSY1* were associated with mixed hearing loss and SNHL, respectively; patients with *MPDZ* mutation had retinal involvement, including foveal dysplasia with a thin inner retina, and SNHL; *EEF1D* patients were reported to have optic atrophy in 3 patients and retinal pigmentary abnormalities in 1. Phenotypic differences could be due to allele type and/or genetic background differences that modify gene function.

One of the human orthologues leading to nonsensory phenotypes is *SLC20A2*, which causes dominant primary familial brain calcification (also known as Fahr's syndrome), a condition that manifests with parkinsonism. The OMIM database has also reported early onset epilepsy, developmental delay, and mental retardation in patients harboring

SLC20A2 mutations. In 1 patient with USH1 and parkinsonism manifested at typical onset (>60 years old), we identified a rare missense variant in this gene, p.Lys72Thr, that is predicted to be likely causal. This variant has never been reported in any patient with Fahr's syndrome, and on ClinVar, the only missense variant affecting the same position (p.Lys72Arg) has been classified as variant of uncertain significance after being reported as part of a commercial genetic panel for inborn genetic diseases. Despite the interesting genetic finding in our patient, the lack of further USH1 patients with variants in *SLC20A2* and its clear association with Fahr's syndrome do not allow us to present this finding fully as a novel genetic association, but rather as a candidate gene for USH1. Therefore, recognizing known disease associations for these candidate genes using existing genetic databases remains a crucial step in validating any novel association and proposing a candidate gene for genetic testing panels.

The literature search on KO and/or HET mouse lines of USH genes and inherited DSI genes revealed that mouse lines of other non-USH inherited DSI genes had higher fidelity regarding retinopathy, suggesting that these genes could affect parts of the photoreceptors that may be similar between humans and mice. This observation supports the conclusion that USH genes likely participate in calyceal processes and the periciliary membrane, which are more prominent in primate photoreceptors than in those of rodents. However, other DSI genes may function in other photoreceptor compartments, which may be more similar among these species. Because our candidate genes frequently had additional phenotypes beyond retinal and hearing abnormalities, we expect that a few genes are responsible for USH, with most being associated with other DSI syndromes.

Investigating the cellular expression of USH genes and our candidate gene set in both species revealed no expression of some of the established USH genes (*USH1G*, *CLRN1*) in either rods or RPE cells of the human retina. Nevertheless, mutation of either of these genes causes RP as part of the USH phenotype. Therefore, we conclude that some bona fide disease-causing genes may escape the resolution of single-cell transcriptomics. Accordingly, the expression of *C1orf116* and *ATP8B1* was detected neither in RPE cells nor in rod photoreceptors. This could be due to a low level of expression or to cell non-autonomous effects; however, the absence of expression of these genes does not preclude a role for them in disease.

Protein interaction analysis of our gene sets revealed 2 interactions between proteins encoded by candidates (DYRK1B and FER) and ciliopathy genes. The dual-specificity tyrosine-regulated kinase (*DYRK*) family and *FER* are both evolutionarily conserved genes.[56,57] Cell proliferation, apoptosis, differentiation, and survival are managed by the DYRK family through altering protein activation status, cellular localization, and turnover.[56] Other DYRKS have been involved in regulating the primary cilium (10.1038/s42003-025-08373-5); DYRK1B modulates the activity and protein stability of GLI transcription factors, which are critical mediators of the Hedgehog signal that operates through primary cilia (10.18632/oncotarget.13662; 10.2337/db25-196-OR). FER is a nontransmembrane receptor tyrosine kinase within the *fes/fps* family with ubiquitous expression.[57] This gene participates in cell survival, cytoskeleton rearrangement, epithelial maintenance, and leukocyte differentiation and chemotaxis.[57] FER is involved in ciliary function and hence may cause DSI. The other 16 candidates we identified do not have predicted interactions with ciliopathy or DSI proteins or with one another at a 0.9 confidence level, despite being expressed in rods and HCs. This finding suggests that this cohort of relatively understudied genes may underlie heretofore unappreciated mechanisms of DSI, such as USH. Accordingly, bioinformatic study pointed to novel functions of candidate genes that were not present among USH and other DSI gene sets. Gene ontology analysis indicated that the candidate gene set is involved in "molecular adaptor activity" (GO:0060090) and "transporter activity" (GO:0005215). These GO terms were not found among existing USH or other DSI gene sets. Subsequent study of candidate genes will elucidate their role in sensory neurons and the degree to which they affect vision and hearing in people.

Through our literature review, we observed that some patients with USH with mutations in the scaffold *USH1C*, which is a confirmed USH1 gene, exhibit severe inflammatory enteropathy and nephropathy along with vision and auditory loss. *USH1C* is shared between the intermicrovillar adhesion complex (IMAC), a complex required for the proper organization of enterocytes' apical microvilli in the form of a brush border, and the USH complex, although the splice isoforms used between the 2 complexes vary.[58] *CALML4*, a novel IMAC component, is highly expressed at the distal tips of enterocytes' microvilli and the stereocilia of HCs, the main action sites of the IMAC and USH complex, respectively. Coimmunoprecipitation experiments in a published study revealed that this gene functions as a light chain by interacting with the neck region of both MYO7B in IMAC and MYO7A in the USH complex.[58] In addition, in a genome-wide linkage screen performed on 2 consanguineous Pakistani families with the USH1 phenotype, *CALML4* is reported within the USH1H locus.[59] Thus, a mutation in this gene may result in USH1H. Future studies on *Calml4* KO mice generated by the IMPC will help clarify this issue.

Studying retinal abnormalities using IMPC mice is complicated by the presence of the *Crb1*^{rd8} variant in C57BL/6N mice, the background on which all IMPC mice were generated,[60] which is associated with a slowly progressive photoreceptor degeneration.[61] To mitigate the number of false positive hits during eye screening, phenotyp-

ing staff were trained to distinguish the background level of retinal dysplasia in *Crb1*^{rd8} mice. The examiners were also masked to the genotype of the mice, and WT mice were mixed in with KO animals. We consider the retinal hits identified by IMPC phenotyping to be a sensitized screen with an overrepresented proportion of lines with abnormal retinas, some of which may be genetic modifiers of *Crb1*.[62] Some of these KO lines may not have any retinal abnormality independent of *Crb1*^{rd8},[50] which is a limitation of this study. To maximize the rigor of this study and minimize the chance of false positive genes, we imposed an additional threshold of only including mouse lines that had bilaterally symmetric retinal findings. Nevertheless, some lines, such as *Fer* and *Eef1d* could not be corroborated with routine histopathologic studies. As all test elements of the IMPC phenotyping process are performed at a single time point, more comprehensive longitudinal evaluation of the *Eef1d* and *Fer* lines may reveal more alterations in retinal and/or inner ear histopathology. Similarly, the onset of symptoms in different types of USH varies from the appearance of RP within the first decade of life and typically congenital SNHL in USH1 patients to the appearance of USH4 symptoms, usually approximately 40 years of age.[2] *EEF1D*[63] and *PIGQ*[64] mutations have been previously associated with retinopathies in patients. Furthermore, ATP8B1 deficiency in patients was reported to cause hearing loss.[43] All were not mentioned in the RetNet, DVD, or SHIELD databases, highlighting the importance of further studies on our candidate genes list.

Our study highlights the power of mouse models to identify novel causative genes for human diseases, including inherited retinopathies and deafness. This strategy contributes to a greater understanding of the related molecular functions and signaling pathways underlying single-gene disorders and promotes enhanced genetic diagnosis. Furthermore, we identified known disease associations of the candidate genes. We advocate using existing genetic databases to further assess any human correlations before adding the candidate genes to genetic testing panels. We would also strongly suggest that this study is an example of discoveries that can be made only by using an in vivo model and that cannot be replaced by a novel alternative methodology or other non-in vivo systems.

CREDIT AUTHORSHIP CONTRIBUTION STATEMENT

ALA MOSHIRI: Data curation, Investigation, Writing – review & editing. **NIUSHA KASIRI:** Data curation, Investigation, Writing – original draft, Writing – review & editing. **MICHAEL SHEA:** Data curation, Investigation, Writing – review & editing. **LAYLA ALI:** Investigation, Writing – review & editing, Data curation. **BENJAMIN YANG:** Data curation, Investigation, Writing – review & editing. **ANDY SHAO:** Data curation, Investigation, Writing – review & editing. **DAVE CLARY:** Data curation, Investigation, Writing – review & editing. **ANN M. FLENNIKEN:** Data curation, Investigation, Writing – review & editing. **MOHAMMAD ESKANDARIAN:** Data curation, Investigation, Writing – review & editing. **OANA V. AMARIE:** Data curation, Investigation, Writing – review & editing. **LORE BECKER:** Data curation, Investigation, Writing – review & editing. **RICCARDO SANGERMANO:** Data curation, Investigation, Writing – review & editing. **EMILY M. PLACE:** Data curation, Investigation, Writing – review & editing. **KINGA M. BUJAKOWSKA:** Data curation, Investigation, Writing – review & editing. **RACHEL M. HUCKFELDT:** Data curation, Investigation, Writing – review & editing. **ZORANA BERBEROVIC:** Data curation, Investigation, Writing – review & editing. **RAPHAËL BOUR:** Data curation, Investigation, Writing – review & editing. **FABRICE RIET:** Data curation, Investigation, Writing – review & editing. **STEVE D. BROWN:** Data curation, Investigation, Writing – review & editing. **ABIGAIL D'SOUZA:** Data curation, Investigation, Writing – review & editing. **HELMUT FUCHS:** Data curation, Investigation, Writing – review & editing. **VALERIE GAILUS-DURNER:** Data curation, Investigation, Writing – review & editing. **ALAIN GUIMOND:** Data curation, Investigation, Writing – review & editing. **YANN HÉRAULT:** Data curation, Investigation, Writing – review & editing. **MARTIN HRABĚ DE ANGELIS:** Data curation, Investigation, Writing – review & editing. **ALINE LUX:** Data curation, Investigation, Writing – review & editing. **CHRISTOPHE MITTELHAEUSER:** Data curation, Investigation, Writing – review & editing. **LAURYL M.J. NUTTER:** Data curation, Investigation, Writing – review & editing. **MARCELA PALKOVA:** Data curation, Investigation, Writing – review & editing. **JIRI LINDOVSKY:** Data curation, Investigation, Writing – review & editing. **BENOIT PETIT-DEMOULIERE:** Data curation, Investigation, Writing – review & editing. **JAN PROCHAZKA:** Data curation, Investigation, Writing – review & editing. **VIVIAN BRADASCHIA:** Data curation, Investigation, Writing – review & editing. **LOIS KELSEY:** Data curation, Investigation, Writing – review & editing. **COLIN MCKERLIE:** Data curation, Investigation, Writing – review & editing. **MILES JOSEPH RAISHBROOK:** Data curation, Investigation, Writing – review & editing. **RADISLAV SEDLACEK:** Data curation, Investigation, Writing – review & editing. **LOUISE LANOUE:** Data curation, Investigation, Writing – review & editing. **K.C. KENT LLOYD:** Data curation, Investigation, Writing – review & editing. **MICHEL J. ROUX:** Data curation, Investigation, Writing – review & editing. **OLIVIA BERMINGHAM-MCDONOGH:** Data curation, Investigation, Writing – review & editing.

Funding/Support: This study received no funding. **Financial Disclosures:** The authors indicate no financial support or conflicts of interest. The authors attest meeting the current ICMJE criteria for authorship.
Acknowledgments: The authors thank all members of the Medical Research Council (MRC) Harwell Institute, Helmholtz Munich (HMGU), Model Animal Research Center (MARC), Institute of Molecular Genetics (IMG), Wellcome Trust Sanger Institute (WTSI), Institut Clinique de la Souris (ICS)—PHENOMIN-ICS, Baylor College of Medicine (BCM), The Jackson Laboratory (JAX), The Center for Phenogenomics (TCP), and University of California, Davis (UC Davis). Work of the HMGU was supported by Infrafrontier grant 01KX1012; EU Horizon2020: IPAD-MD funding 653961 (MHdA). The authors used services of the Czech Centre for Phenogenomics at the IMG, supported by the Czech Academy of Sciences RVO 68378050 and by the projects LM2023036, CZ.02.1.01/0.0/0.0/ 16_013/0001789, and CZ.02.1.01/0.0/0.0/18_046/0015861, provided by the Ministry of Education, Youth and Sports of the Czech Republic. The work of PHENOMIN-ICS was supported in part by IdEx Unistra (ANR-10-IDEX-0002), SFRI-STRAT'US project (ANR-20-SFRI-0012), and INBS PHENOMIN (ANR-10-IDEX-0002-02) under the framework of the France 2030 Program to YH. In addition, this work was supported by grants from the National Eye Institute (R01EY035717 [KMB] and P30EY014104 [MEEI core support]), Iraty Award 2023 (KMB), Lions Foundation (KMB), Research to Prevent Blindness Unrestricted Grant (KMB), the Curing Kids Foundation (KMB), and Foundation Fighting Blindness Career Development Award (RMH).
The authors also thank the patients and their family members for their participation in this study and the Ocular Genomics Institute Genomics Core members for their experimental assistance.

REFERENCES

1. Swenor BK, Ramulu PY, Willis JR, Friedman D, Lin FR. The prevalence of concurrent hearing and vision impairment in the United States. *JAMA Intern Med*. 2013;173(4):312–313. doi:10.1001/jamainternmed.2013.1880.
2. Guimaraes TAC de, Arram E, Shakarchi AF, Georgiou M, Michaelides M. Inherited causes of combined vision and hearing loss: clinical features and molecular genetics. *Br J Ophthalmol*. 2023;107(10):1403–1414. doi:10.1136/bjo-2022-321790.
3. Mathur P, Yang J. Usher syndrome: hearing loss, retinal degeneration and associated abnormalities. *Biochim Biophys Acta Mol Basis Dis*. 2015;1852(3):406–420. doi:10.1016/j.bbadis.2014.11.020.
4. Delmaghani S, El-Amraoui A. The genetic and phenotypic landscapes of Usher syndrome: from disease mechanisms to a new classification. *Hum Genet*. 2022;141(3-4):709. doi:10.1007/s00439-022-02448-7.
5. Fuster-García C, García-Bohórquez B, Rodríguez-Muñoz A, et al. Usher syndrome: genetics of a human ciliopathy. *Int J Mol Sci*. 2021;22(13):6723. doi:10.3390/ijms22136723.
6. Castiglione A, Möller C. Usher syndrome. *Audiol Res*. 2022;12(1):42–65. doi:10.3390/audiolres12010005.
7. Sahly I, Dufour E, Schietroma C, et al. Localization of Usher 1 proteins to the photoreceptor calyceal processes, which are absent from mice. *J Cell Biol*. 2012;199(2):381–399. doi:10.1083/jcb.201202012.
8. Williams DS. Usher syndrome: animal models, retinal function of Usher proteins, and prospects for gene therapy. *Vision Res*. 2007;48(3):433. doi:10.1016/j.visres.2007.08.015.
9. Groza T, Gomez FL, Mashhadi HH, et al. The International Mouse Phenotyping Consortium: comprehensive knockout phenotyping underpinning the study of human disease. *Nucleic Acids Res*. 2023;51(D1):D1038–D1045. doi:10.1093/nar/gkac972.
10. Dickinson ME, Flenniken AM, Ji X, et al. High-throughput discovery of novel developmental phenotypes. *Nature*. 2016;537(7621):508–514. doi:10.1038/nature19356.
11. Birling MC, Yoshiki A, Adams DJ, et al. A resource of targeted mutant mouse lines for 5,061 genes. *Nat Genet*. 2021;53(4):416–419. doi:10.1038/s41588-021-00825-y.
12. Elrick H, Peterson KA, Willis BJ, et al. Impact of essential genes on the success of genome editing experiments generating 3313 new genetically engineered mouse lines. *Sci Rep*. 2024;14(1):22626. doi:10.1038/s41598-024-72418-8.
13. Bowl MR, Simon MM, Ingham NJ, et al. A large scale hearing loss screen reveals an extensive unexplored genetic landscape for auditory dysfunction. *Nat Commun*. 2017;8(1):886. doi:10.1038/s41467-017-00595-4.
14. Moore BA, Leonard BC, Sebbag L, et al. Identification of genes required for eye development by high-throughput screening of mouse knockouts. *Commun Biol*. 2018;1:236. doi:10.1038/s42003-018-0226-0.
15. Haselimashhadi H, Mason JC, Mallon AM, Smedley D, Meehan TF, Parkinson H. OpenStats: A robust and scalable software package for reproducible analysis of high-throughput phenotypic data. *PLoS One*. 2020;15(12):e0242933. doi:10.1371/journal.pone.0242933.
16. Percie du Sert N, Hurst V, Ahluwalia A, et al. The ARRIVE guidelines 2.0: updated guidelines for reporting animal research. *PLoS Biol*. 2020;18(7):e3000410. doi:10.1371/journal.pbio.3000410.
17. Stelzer G, Rosen N, Plaschkes I, et al. The GeneCards suite: from gene data mining to disease genome sequence analyses. *Curr Protoc Bioinform*. 2016;54(1):1.30.1–1.30.33. doi:10.1002/cpbi.5.
18. Safran M, Rosen N, Twik M, et al. The GeneCards suite. In: Abugessaisa I, Kasukawa T, eds. *Practical Guide to Life Science Databases* Springer Nature; 2021:27–56. doi:10.1007/978-981-16-5812-9_2.
19. Szklarczyk D, Kirsch R, Koutrouli M, et al. The STRING database in 2023: protein—protein association networks and functional enrichment analyses for any sequenced genome of interest. *Nucleic Acids Res*. 2022;51(D1):D638–D646. doi:10.1093/nar/gkac1000.
20. Doncheva NT, Morris JH, Gorodkin J, Jensen LJ. Cytoscape StringApp: network analysis and visualization of proteomics data. *J Proteome Res*. 2019;18(2):623–632. doi:10.1021/acs.jproteome.8b00702.
21. Thomas PD, Ebert D, Muruganujan A, Mushayahama T, Albou LP, Mi H. PANTHER: making genome-scale phylogenetics accessible to all. *Protein Sci*. 2022;31(1):8–22. doi:10.1002/pro.4218.
22. Mi H, Muruganujan A, Huang X, et al. Protocol Update for large-scale genome and gene function analysis with the PANTHER classification system (v.14.0). *Nat Protoc*. 2019;14(3):703–721. doi:10.1038/s41596-019-0128-8.

23. Huang DW, Sherman BT, Lempicki RA. Systematic and integrative analysis of large gene lists using David bioinformatics resources. *Nat Protoc*. 2009;4(1):44–57. doi:10.1038/nprot.2008.211.
24. Huang DW, Sherman BT, Lempicki RA. Bioinformatics enrichment tools: paths toward the comprehensive functional analysis of large gene lists. *Nucleic Acids Res*. 2009;37(1):1–13. doi:10.1093/nar/gkn923.
25. Swamy VS, Fufa TD, Hufnagel RB, McGaughey DM. Building the mega single-cell transcriptome ocular meta-atlas. *GigaScience*. 2021;10(10):giab061. doi:10.1093/gigascience/giab061.
26. Orvis J, Gottfried B, Kancherla J, et al. gEAR: gene Expression Analysis Resource portal for community-driven, multi-omic data exploration. *Nat Methods*. 2021;18(8):843–844. doi:10.1038/s41592-021-01200-9.
27. van der Valk WH, van Beelen ESA, Steinhart MR, et al. A single-cell level comparison of human inner ear organoids with the human cochlea and vestibular organs. *Cell Rep*. 2023;42(6):112623. doi:10.1016/j.celrep.2023.112623.
28. Daiger SP, Rossiter BJ, Greenberg J, Christoffels A, Hide W. Data services and software for identifying genes and mutations causing retinal degeneration. *Invest Ophthalmol Vis Sci*.. 1998;39(suppl):S295.
29. Shen J, Scheffer DI, Kwan KY, Corey DP. SHIELD: an integrative gene expression database for inner ear research *[Database]*. *J Biol Databases Curation*. 2015;2015:bav071. doi:10.1093/database/bav071
30. Azaiez H, Booth KT, Ephraim SS, et al. Genomic landscape and mutational signatures of deafness-associated genes. *Am J Hum Genet*.. 2018;103(4):484–497. doi:10.1016/j.ajhg.2018.08.006.
31. Higgins K, Moore BA, Berberovic Z, et al. Analysis of genome-wide knockout mouse database identifies candidate ciliopathy genes. *Sci Rep*. 2022;12(1):20791. doi:10.1038/s41598-022-19710-7.
32. Scott HA, Place EM, Ferenchak K, et al. Expanding the phenotypic spectrum in RDH12-associated retinal disease. *Cold Spring Harb Mol Case Stud*. 2020;6(1):a004754. doi:10.1101/mcs.a004754.
33. Moye AR, Bedoni N, Cunningham JG, et al. Mutations in ARL2BP, a protein required for ciliary microtubule structure, cause syndromic male infertility in humans and mice. *PLoS Genet*. 2019;15(8):e1008315. doi:10.1371/journal.pgen.1008315.
34. Haer-Wigman L, Newman H, Leibu R, et al. Non-syndromic retinitis pigmentosa due to mutations in the mucopolysaccharidosis type IIIC gene, heparan-alpha-glucosaminide N-acetyltransferase (HGSNAT). *Hum Mol Genet*. 2015;24(13):3742–3751. doi:10.1093/hmg/ddv118.
35. Men CJ, Bujakowska KM, Comander J, et al. The importance of genetic testing as demonstrated by two cases of CACNA1F-associated retinal generation misdiagnosed as LCA. *Mol Vis*. 2017;23:695–706.
36. Collins RL, Brand H, Karczewski KJ, et al. A structural variation reference for medical and population genetics. *Nature*. 2021;581:444–451 Published correction appears in *Nature*.;590(7846):E55. d oi:10.1038/s41586-020-03176-6. doi:10.1038/s41586-020-2287-8.
37. Lewandowski D, Foik AT, Smidak R, et al. Inhibition of ceramide accumulation in AdipoR1-/- mice increases photoreceptor survival and improves vision. *JCI Insight*. 2022;7(4):e156301. doi:10.1172/jci.insight.156301.
38. Macke EL, Henningsen E, Jessen E, et al. Loss of chondroitin sulfate Modification Causes Inflammation and Neurodegeneration in skt Mice. *Genetics*. 2020;214(1):121–134. doi:10.1534/genetics.119.302834.
39. Liu Y, Xu L, Hennig AK, et al. Liver-directed neonatal gene therapy prevents cardiac, bone, ear, and eye disease in mucopolysaccharidosis I mice. *Mol Ther*. 2005;11(1):35–47. doi:10.1016/j.ymthe.2004.08.027.
40. Albrecht NE, Alevy J, Jiang D, et al. Rapid and integrative discovery of retina regulatory molecules. *Cell Rep*.. 2018;24(9):2506–2519. doi:10.1016/j.celrep.2018.07.090.
41. Yu J, Lei K, Zhou M, et al. KASH protein Syne-2/Nesprin-2 and SUN proteins SUN1/2 mediate nuclear migration during mammalian retinal development. *Hum Mol Genet*. 2011;20(6):1061–1073. doi:10.1093/hmg/ddq549.
42. Karanjawala ZE, Hinton DR, Oh E, Hsieh CL, Lieber MR. Developmental retinal apoptosis in Ku86−/− mice. *DNA Repair (Amst)*. 2003;2(12):1429–1434. doi:10.1016/j.dnarep.2003.08.011.
43. Stapelbroek JM, Peters TA, van Beurden DH, et al. ATP8B1 is essential for maintaining normal hearing. *Proc Natl Acad Sci U S A*. 2009;106(24):9709–9714. doi:10.1073/pnas.0807919106.
44. Schachern PA, Cureoglu S, Tsuprun V, Paparella MM, Whitley CB. Age-related functional and histopathological changes of the ear in the MPS I mouse. *Int J Pediatr Otorhinolaryngol*. 2007;71(2):197–203. doi:10.1016/j.ijporl.2006.09.016.
45. Jarysta A, Tarchini B. Multiple PDZ domain protein maintains patterning of the apical cytoskeleton in sensory hair cells. *Development*. 2021;148(14):dev199549. doi:10.1242/dev.199549.
46. Horn HF, Brownstein Z, Lenz DR, et al. The LINC complex is essential for hearing. *J Clin Invest*. 2013;123(2):740–750. doi:10.1172/JCI66911.
47. Campbell T, Lou X, Slone J, et al. Mitochondrial genome variant m.3250T>C as a possible risk factor for mitochondrial cardiomyopathy. *Hum Mutat*. 2021;42(2):177–188. doi:10.1002/humu.24143.
48. Teng YN, Wang TR, Hwu WL, Lin SP, Lee-Chen GJ. Identification and characterization of -3c-g acceptor splice site mutation in human alpha-L-iduronidase associated with mucopolysaccharidosis type IH/S. *Clin Genet*. 2000;57(2):131–136. doi:10.1034/j.1399-0004.2000.570207.x.
49. Schrauwen I, Melegh BI, Chakchouk I, et al. Hearing impairment locus heterogeneity and identification of PLS1 as a new autosomal dominant gene in Hungarian Roma. *Eur J Hum Genet*. 2019;27(6):869–878. doi:10.1038/s41431-019-0372-y.
50. Kwon YS, Tham A, Lopez AJ, et al. Cytoglobin deficiency potentiates Crb1-mediated retinal degeneration in rd8 mice. *Dev Biol*. 2019;458(2):141. doi:10.1016/j.ydbio.2019.10.013.
51. Morisada N, Hamada R, Miura K, et al. Bardet—Biedl syndrome in two unrelated patients with identical compound heterozygous SCLT1 mutations. *CEN Case Rep*. 2020;9(3):260–265. doi:10.1007/s13730-020-00472-y.
52. Wang C, Li Y, Shi L, et al. Mutations in SLC20A2 link familial idiopathic basal ganglia calcification with phosphate

homeostasis. *Nat Genet*. 2012;44(3):254–256. doi:10.1038/ng.1077.
53. Karczewski KJ, Francioli LC, Tiao G, et al. The mutational constraint spectrum quantified from variation in 141,456 humans. *Nature*. 2020;581(7809):434–443. doi:10.1038/s41586-020-2308-7.
54. Fokkema IFAC, Kroon M, López Hernández JA, et al. The LOVD3 platform: efficient genome-wide sharing of genetic variants. *Eur J Hum Genet*. 2021;29(12):1796–1803. doi:10.1038/s41431-021-00959-x.
55. Landrum MJ, Lee JM, Riley GR, et al. ClinVar: public archive of relationships among sequence variation and human phenotype. *Nucleic Acids Res*. 2014;42:D980–D985. doi:10.1093/nar/gkt1113.
56. Yoshida S, Yoshida K. New insights into the roles for DYRK family in mammalian development and congenital diseases. *Genes Dis*.. 2022;10(3):758. doi:10.1016/j.gendis.2021.12.004.
57. Dolgachev VA, Goldberg R, Suresh MV, et al. Electroporation-mediated delivery of the FER gene in the resolution of trauma-related fatal pneumonia. *Gene Ther*. 2016;23(11):785–796. doi:10.1038/gt.2016.58.
58. Choi MS, Graves MJ, Matoo S, et al. The small EF-hand protein CALML4 functions as a critical myosin light chain within the intermicrovillar adhesion complex. *J Biol Chem*. 2020;295(28):9281–9296. doi:10.1074/jbc.RA120.012820 .
59. Ahmed ZM, Riazuddin S, Khan SN, Friedman PL, Riazuddin S, Friedman TB. USH1H, a novel locus for type I Usher syndrome, maps to chromosome 15q22-23. *Clin Genet*. 2009;75(1):86–91. doi:10.1111/j.1399-0004.2008.01038.x.
60. Moore BA, Roux MJ, Sebbag L, et al. A population study of common ocular abnormalities in C57BL/6N rd8 mice. *Invest Ophthalmol Vis Sci*. 2018;59(6):2252–2261. doi:10.1167/iovs.17-23513.
61. Mattapallil MJ, Wawrousek EF, Chan CC, et al. The Rd8 mutation of the Crb1 gene is present in vendor lines of C57BL/6N mice and embryonic stem cells, and confounds ocular induced mutant phenotypes. *Invest Ophthalmol Vis Sci*. 2012;53(6):2921–2927. doi:10.1167/iovs.12-9662.
62. Weatherly SM, Collin GB, Charette JR, et al. Identification of Arhgef12 and Prkci as genetic modifiers of retinal dysplasia in the Crb1rd8 mouse model. *PLoS Genet*. 2022;18(6):e1009798. doi:10.1371/journal.pgen.1009798.
63. Averdunk L, Al-Thihli K, Surowy H, et al. Expanding the spectrum of EEF1D neurodevelopmental disorders: biallelic variants in the guanine exchange domain. *Clin Genet*. 2023;103(4):484–491. doi:10.1111/cge.14290.
64. Johnstone DL, Nguyen TTM, Zambonin J, et al. Early infantile epileptic encephalopathy due to biallelic pathogenic variants in PIGQ: report of seven new subjects and review of the literature. *J Inherit Metab Dis*. 2020;43(6):1321–1332. doi:10.1002/jimd.12278.